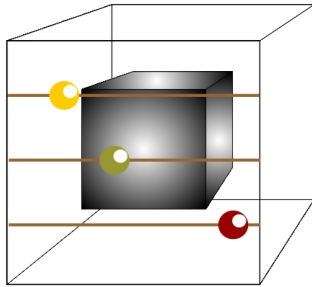


anatabacus v1.1:
calculator for image distortions



for BrainVoyager QX

Contents

1	Manual for EPI distortion correction plugin for BrainVoyager	4
1.1	Introduction	4
1.2	Installation of the plugin	5
1.3	Activation of the plugin	5
1.4	Data requirements	6
1.5	History, present and future	7
1.5.1	Planned features	7
1.5.2	Known issues	7
1.5.3	Notes on plugin versions	7
1.6	Acknowledgements	7
1.7	Main menu of anatabacus	8
1.8	Creating a VMR-based mask	10
1.8.1	Introduction	10
1.8.2	Brain extraction	10
1.8.3	Map VMR to FMR	11
1.9	Unwrapping of the differential phase map	12
1.9.1	Introduction	12
1.9.2	Usage	13
1.9.3	Background	15
1.10	Collect acquisition parameters	17
1.10.1	Introduction	17
1.10.2	Usage	17
1.10.3	Background	19
1.11	Coregistration	22
1.11.1	Introduction	22
1.11.2	Usage	22
1.11.3	Background	22
1.12	Creating a field inhomogeneity map	23
1.12.1	Usage	23
1.12.2	Background	24
1.13	Calculate pixel shift map	25
1.13.1	Usage	25
1.13.2	Background	27
1.14	Undistort functional data with pixel shift map	28
1.14.1	Usage	28
1.14.2	Extent of the distortion	30
1.14.3	Background	31
1.15	Evaluation utility (create difference image)	32
1.15.1	Usage	32
1.15.2	Evaluation via coregistration with anatomy	33
1.16	Conversion utilities	35
1.16.1	Conversions: to SI units	36

1.16.2	Conversions: between Cartesian and polar coordinates	39
1.16.3	Conversions: other calculations	42
1.16.4	Background	45
A	Acquisition of B0 field maps	46
A.1	Introduction	46
A.2	Phase map types	46
A.2.1	Spin-echo (SE) phase maps	46
A.2.2	Gradient-echo (GRE) phase maps	46
A.3	Acquisition of phase field maps	47
A.3.1	Acquisition on Bruker scanners	47
A.3.2	Acquisition on Philips scanners	47
A.3.3	Acquisition on General Electric (GE) scanners	47
A.3.4	Acquisition on Siemens Allegra 3T scanner	48
A.4	Manually creating a differential phase map from two phase images with different echo times	50
B	Summary of coordinate systems in MRI	51
B.1	Coordinate systems in Magnetic Resonance Imaging	52
C	Preventive measures	53
C.1	Reducing susceptibility artifacts	53
C.1.1	Global measures	53
C.1.2	Region-specific measures	55
D	Nomenclature	57
D.1	Nomenclature	57
E	Phase wraps and unwrapping	59

Chapter 1

Manual for EPI distortion correction plugin for Brain Voyager

1.1 Introduction

This is the manual for `anatabacus`, a geometrical distortions calculator for BrainVoyager QX (see Goebel et al, 2006 [15]). This plugin makes it possible to apply EPI distortion correction using the pixelshift algorithm (Jezzard Balaban, 1995; [22]), for images that are geometrically distorted due to the susceptibility artifact. This approach requires fieldmaps (either phase and magnitude or real and imaginary), being acquired before the functional run. This routine uses affine transformation code by Thevenaz et al (2000, [35]).

Secondly, a difference image of two fMRIs can be created to evaluate the undistortion/unwarping result visually.

Finally, some calculations can be made as well with this plugin, for example to compute the phase encoding bandwidth or to convert between radians and degrees; also Cartesian (real and imaginary) fieldmaps can be converted to polar coordinates (phase and magnitude).

The EPI distortion correction can be useful for finding the ‘true’ location of a signal, or make the functional image better fit on the anatomical image, and for increasing the power in group studies (see Cusack et al, 2003 [8]). It can not recover lost signal. Preventive measures like proper slice or head positioning, however, can reduce the distortion caused by the susceptibility artifact (see Weiskopf et al, 2006 [36] for reduction of signal loss (“dropout”); Appendix C).

The reference for this plugin is Breman et al (2009; [6]). Its poster can be found via the following link to the BrainVoyager support page PDF.

1.2 Installation of the plugin

To install the plugin, put the `anatabacus_vxxx.dll/dylib/so`, the `anatabacus.ui` and `anatabacus.js` files in the folder
/ (My) documents/BVQXExtensions/Plugins_32 (64) / (see figure 1.1).

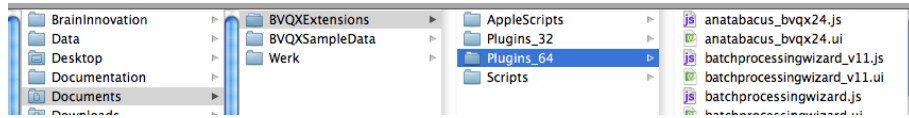


Figure 1.1: Folder to place the plugin

After this has been performed, start BrainVoyager QX.

1.3 Activation of the plugin

Start BrainVoyager QX. To activate the plugin, choose 'anatabacus' from the BrainVoyager QX menu (see figure 1.2).

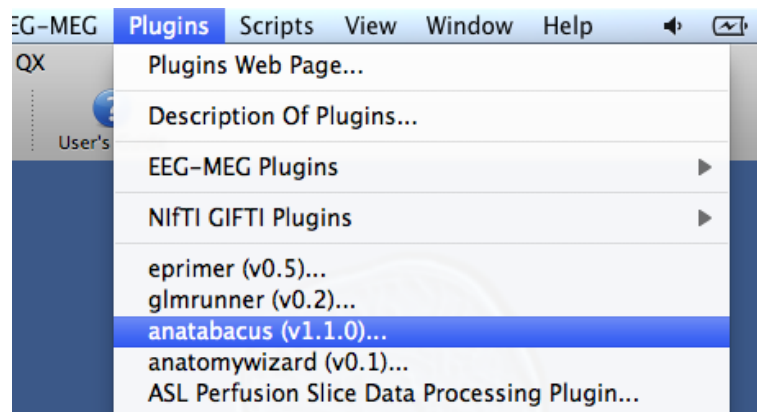


Figure 1.2: Activating the toolbox

A menu will appear where the calculation step(s) can be chosen, the image acquisition parameters can be entered and the files be loaded (see section 1.7).

1.4 Data requirements

Here is briefly summarised how the data should be presented to the plugin:

- If the fieldmap has different measurement parameters as the EPI data, an anatomical image should be available for the coregistration procedure.
- A VMR-based FMR image is recommended for the masking (see section 1.8).
- The phase and magnitude FMR projects should be in float datatype (see figure 1.3).
- After processing, any still attached AMRs should be detached from the undistorted EPI and B0/pixelshift files.

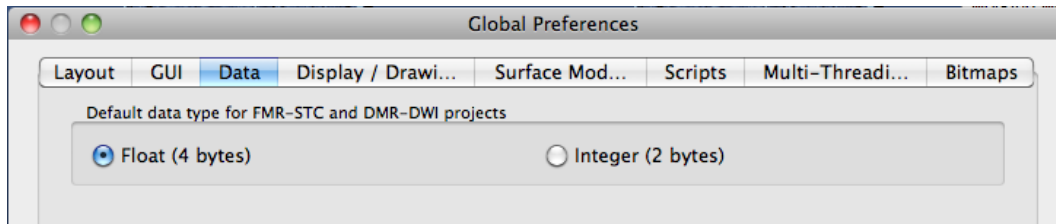


Figure 1.3: Changing the FMR datatype to float in BrainVoyager via 'Global Preferences'

1.5 History, present and future

1.5.1 Planned features

The features described below are not available in this plugin. They might be available in future versions (or not).

- *Include correction for interaction with head motion (“dynamic fieldmaps”).* This is not yet possible with the current version, in *anatabacus* a single, static fieldmap is used to correct all volumes in one run. If also correction for interaction with head motion is required, please see the toolbox of Hutton et al (2004, [19]) and Andersson et al (2003; [1]); see also Sutton et al (2004; [34]).

1.5.2 Known issues

In version 1.0 and 1.1, the AMR files are upside down.

1.5.3 Notes on plugin versions

Notes on version 1.1

A coregistration function has been added for different orientations. Also, the ‘partial Fourier’ in the calculation of the bandwidth in phase encoding direction has been replaced by ‘acceleration factor’. Smoothing after phase unwrapping and calculation of the fieldmap has been added. *March 2014*

Notes on version 1.0

A relaxation method for phase unwrapping has been added (see section 1.9). *October 2011*

Notes on version 0.9

A resampling function for pixelshift maps has been added (see section 1.14). *October 2011*

Notes on version 0.7

The plugin has an Evaluation tab (see section 1.15) and a Conversions tab (see section 1.16).

Notes on version 0.6

The plugin now has a GUI and is updated to BrainVoyager QX 2.2.

Notes on version 0.5

This version includes a full multigrid (FMG) algorithm to unwrap differential phase images.

1.6 Acknowledgements

Many thanks to John Ashburner for contributions on the unwrapping and to Judith Peters, Martin Frost, Sanae Okamoto-Barth, Jochen Weber, Fabrizio Esposito, Judith Eck, Matthew Patten, Matthew Dexter and Federico de Martino for data.

Hester Breman, Joost Mulders and Rainer Goebel

1.7 Main menu of anatabacus

The main menu (see figure 1.4) appears when selecting the ‘anatabacus’ plugin from the BrainVoyager QX ‘Plugins’ menu.

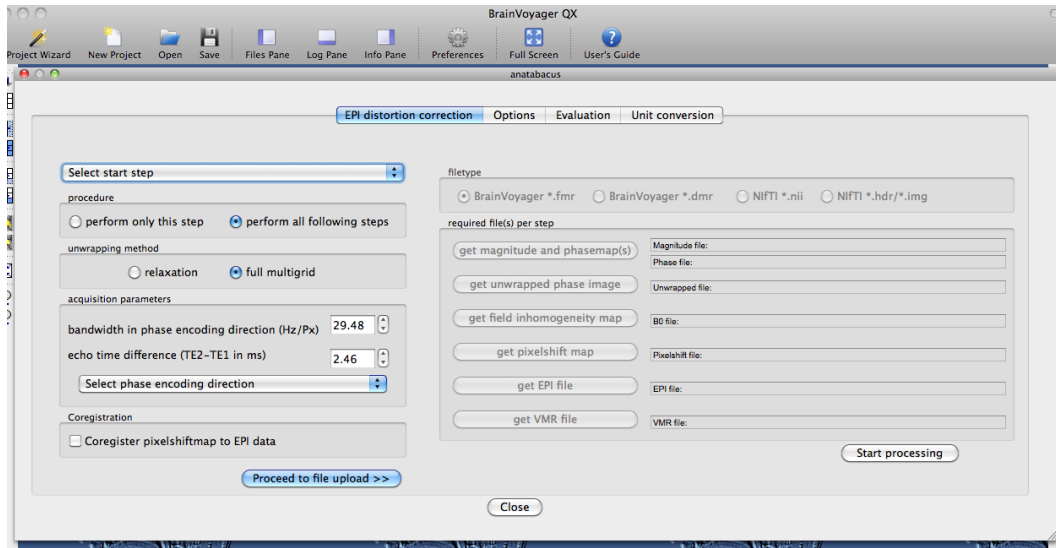


Figure 1.4: Menu of fieldmap correction options

First, one can unwrap the phase map, which is done when there are strongly visible edges in the phase image instead of smooth transitions. It is possible here that jumps between values have been introduced and they should be corrected before using the phase data. Please consult section 1.9 for information about this option.

Using the unwrapped smoothed differential phase map, the field inhomogeneity can be computed (see section 1.12).

Via the next option a pixel shift map can be computed (see section 1.13).

As a last step, the pixel shift map can be used to undistort the EPI image. The procedure is described in section 1.14.

It is possible to perform all following steps after the currently selected steps (radiobuttons for this option are present on the left side of the dialog).

The stages of the fieldmap are shown in figure 1.5. Please note that the black and white appearance of the phase image in radians and the pixelshift map is only a display issue (since the phase in radians have small values, while the usual display of FMR projects is adjusted to intensities of several thousands).

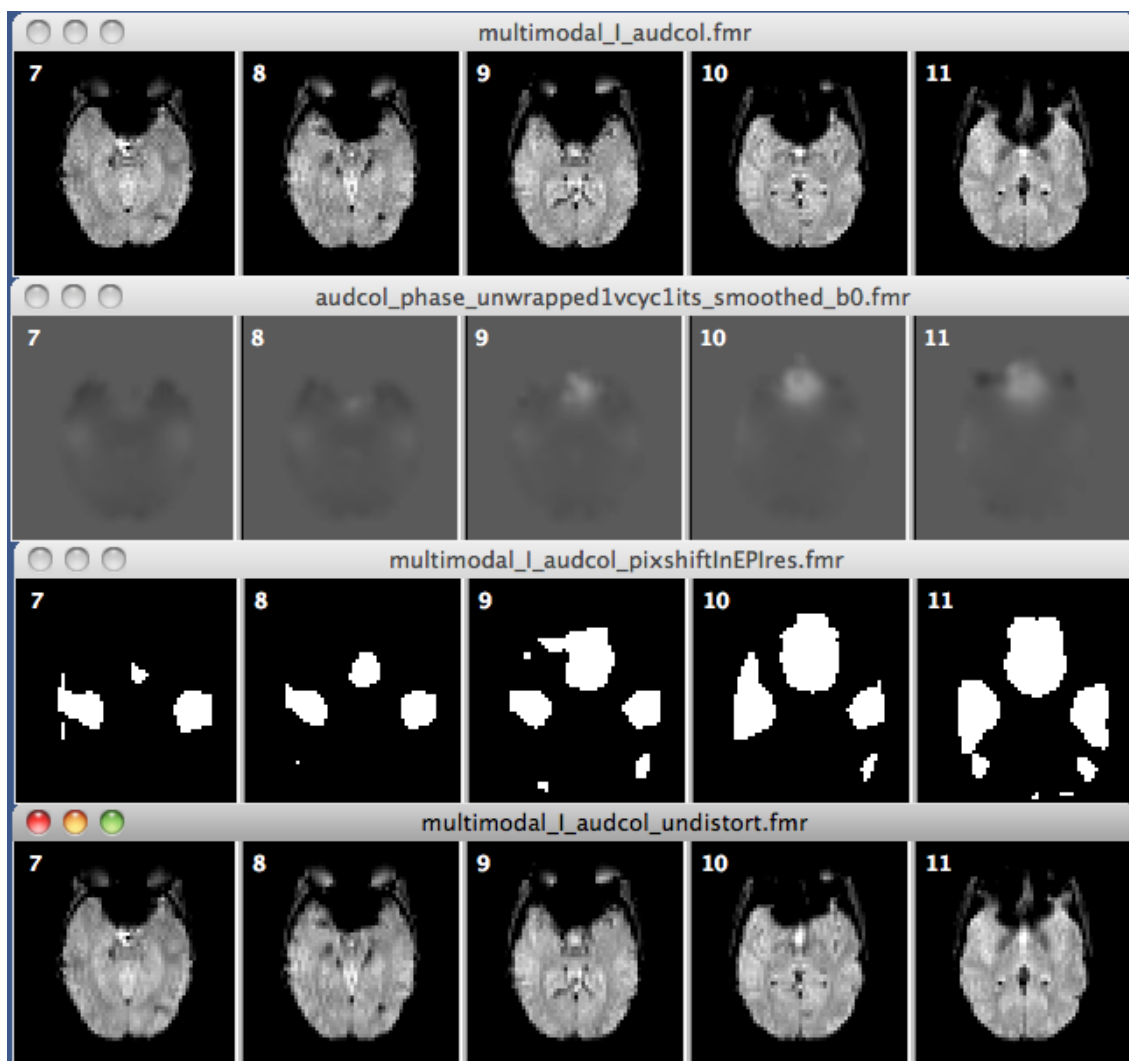


Figure 1.5: Images of all stages of the fieldmap

1.8 Creating a VMR-based mask

1.8.1 Introduction

Since anatabacus v1.1, it is recommended to use an brain extracted-VMR based magnitude (*.fmr) image instead of just the magnitude image; this should be beneficial for the masking of the unwrapped phase image. In the procedure below is described how to create such an image. In future versions, (parts of) the procedure will be automated.

1.8.2 Brain extraction

Use the VMR (which is also necessary in case one needs to coregister the fieldmap to the functional data in anatabacus) or a VMR of the magnitude image, in case no other anatomical scans are available. In BrainVoyager, go to Volumes > Segregate Head from Brain Tissue(see figure 1.6). Save the image with a new extension, like "_BRAIN.vmr" via File > Save As.

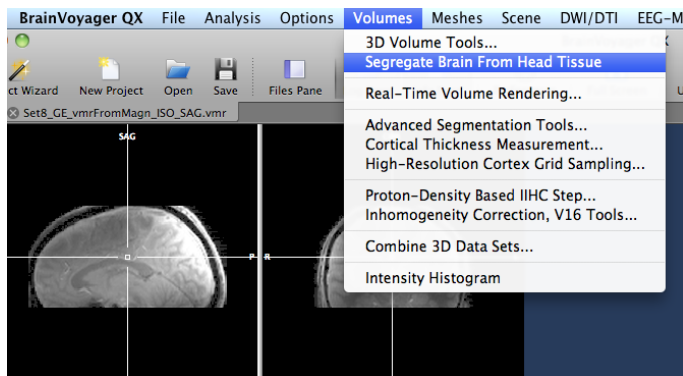


Figure 1.6: Brain extraction

1.8.3 Map VMR to FMR

Use the `fmr2vmrplugin` to map the brain extracted VMR to the magnitude FMR via `Plugins > fmr2vmrplugin` (see figure 1.7).

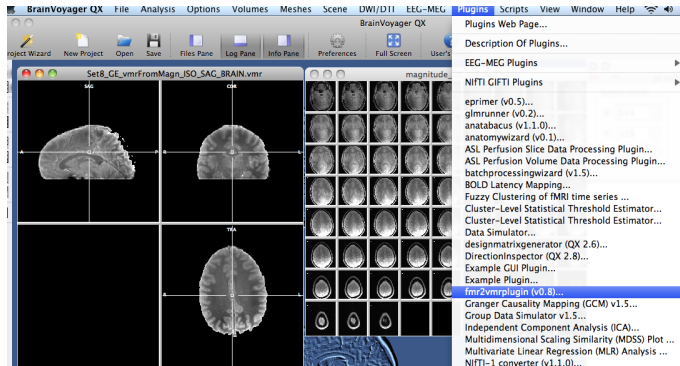


Figure 1.7: Activate `fmr2vmrplugin`

Choose option 2: VMR \rightarrow FMR (see figure 1.8).

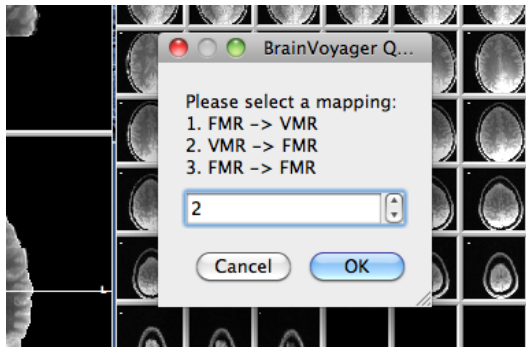


Figure 1.8: Select 'map VMR to FMR'

Reload the `*_VMR_fmri` image to see the effect (see figure 1.9).

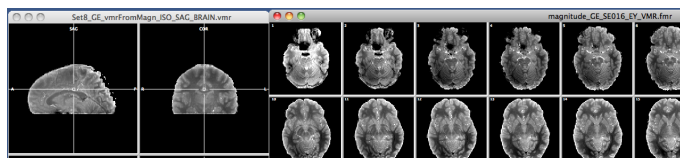


Figure 1.9: Result

1.9 Unwrapping of the differential phase map

1.9.1 Introduction

Sometimes phase jumps (“wraps”) occur when the time between two echoes in the field map (‘phase evolution’) is relatively long. In images, these phase jumps shows as sharp edges; see figure 1.10 for an example of wrapped phase data.

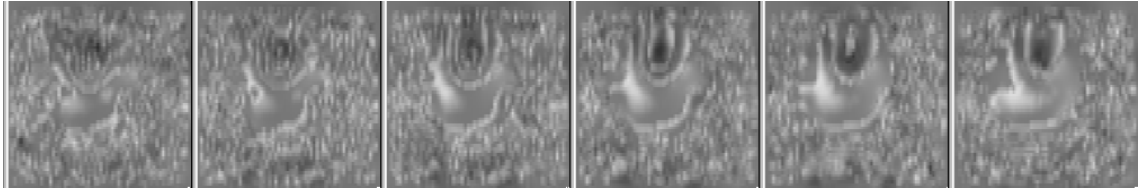


Figure 1.10: Wrapped image (AMR)

Some phase images hardly contain wraps anymore; in for examples results from the `gre_field_mapping` sequence from Siemens are good, since the time between measuring the two phase images is kept short (2.46 ms), so not so much decay occurs. Therefore, in the resulting differential phase map that one obtains from Siemens’ `gre_field_mapping` sequence, usually there are hardly any wraps. But in case there are many phase jumps, it might be good to perform unwrapping, otherwise the fieldmap is not such a useful source of information for undistorting the EPI image.

1.9.2 Usage

Start the `anatabacus` plugin from the BrainVoyager QX “Plugins” menu. In the `startstep` dropdownbox, select “Unwrap” (see figure 1.11).

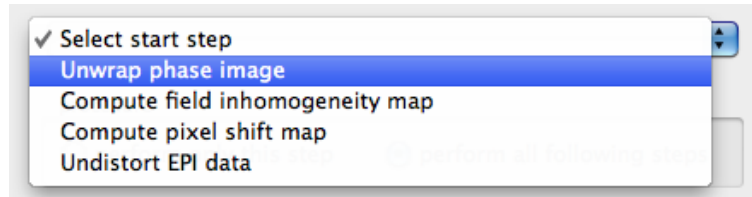


Figure 1.11: In the dropdownbox, select “Unwrap”

For few or no wraps, the 3DFMG method can be applied with default settings (1 cycle and 1 iteration); for other cases, the relaxation method can be used (see figure 1.12). Other considerations could be system resources, since 3DFMG might cause (ungraceful) degradation¹ if the amount of memory in the computer is not enough; in that case, please select the ‘relaxation’ option. Furthermore, the relaxation option seem to produce more conservative maps².

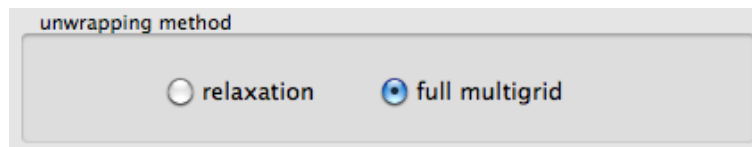


Figure 1.12: Unwrapping options

Then, select - using the radiobuttons - whether to perform all following steps as well or just to unwrap the phase image (see figure 1.13). A file dialog will appear not only to select the differential phase image, but also for an image that can be used as mask. Both images are expected to be in BrainVoyager’s FMR file format.

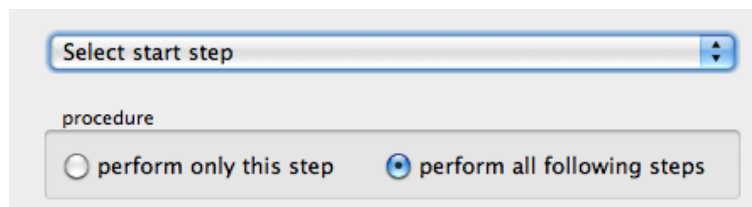


Figure 1.13: Choose to perform only this step or all following steps

Click the button “Proceed to file upload”. A phase and magnitude image button will be activated (see figure 1.15 on the right for a phase image). The phase and magnitude data should contain only one volume (the EPI data can have any number of volumes). Instead of the magnitude image, one could use a brain-extracted VMR that has been projected in the magnitude image (see section 1.8). If the option to perform all steps is chosen, also the “Get EPI button” will be activated, and an EPI needs to be selected as well.

¹= crash

²= smaller pixelshifts

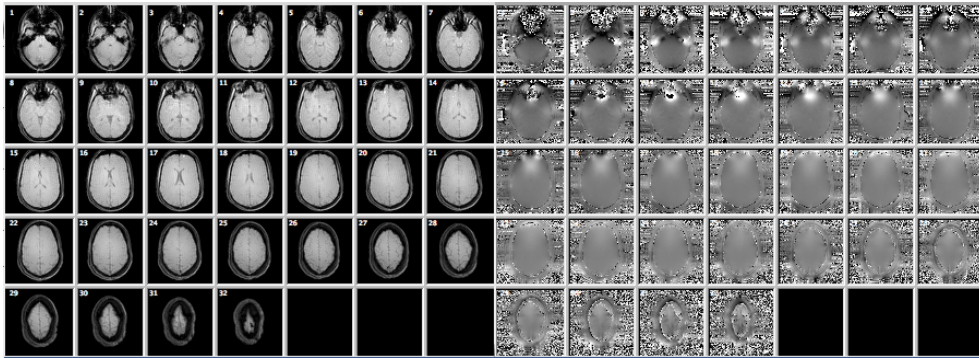


Figure 1.14: Magnitude (left) and phase (right) images created in BrainVoyager as *.fmr projects with 1 volume

When the files are selected, the files are opened in BrainVoyager and the file-names are visible on the dialog.

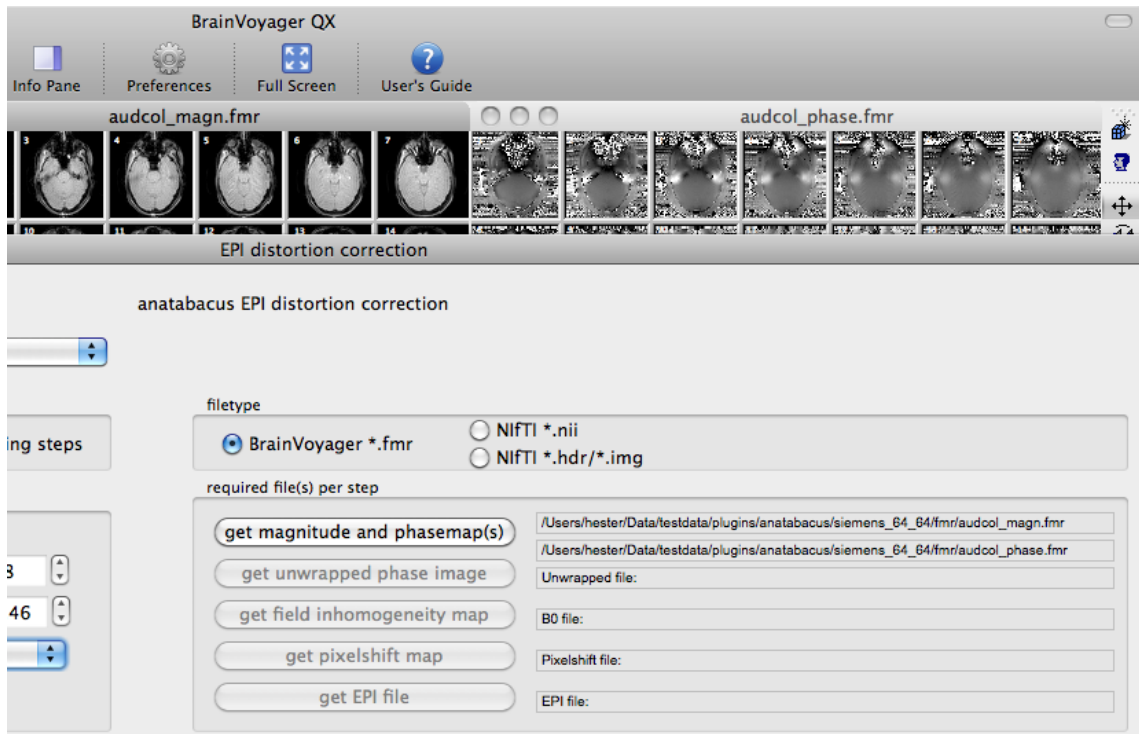


Figure 1.15: Button activated for unwrapping step

In case only unwrapping is performed, click the “Start processing” button. Otherwise, the acquisition parameters have to be provided first. The resulting files are saved as FMR and AMR. The AMR contains a scaled version of the FMR data for display purposes, since the phase data in radians in the FMR are shown in black and white in BrainVoyager (FMR data between $-\pi$ and π appear in black and white).

1.9.3 Background

Scaling to radians

First, the data are scaled to radians: between π and $-\pi$, because - at least for Siemens DICOM - the phase images have intensities between 0 and 4092. The scaling procedure is based on the linear transformation formula which is described in Nijdam & Van Buuren (1994, [26, Ch.6]). It is implemented in the following way:

```
float range = max + fabs(min);  
float newrange = newmax + fabs(newmin);  
float p = (newrange/range);  
float q = newmin - p * min;  
tmp2 = p * vol[i] + q;
```

Unwrapping

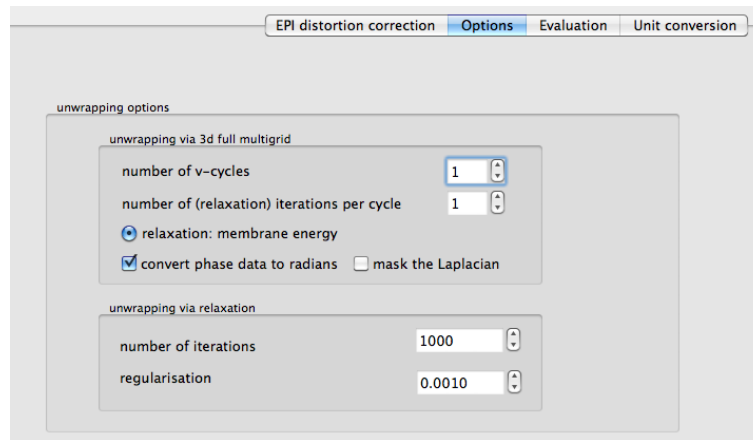


Figure 1.16: Possibility for adjusting the unwrapping parameters via the 'Options' tab

3DFMG: The number of V-cycles and iterations can be adjusted via the spinboxes (see figure 1.16) on the 'Options' tab. The default for number of V-cycles and iterations (see section E) is both 1 and should be fine for most cases. The number of V-cycles and iterations is saved in the filename using abbreviations 'cycl' and 'its' respectively:

<image name>_unwrapped<number>cycl<number>its_*.fmr.

Relaxation: The relaxation method can be summarised as follows [29, Ch.17]:

An initial solution is guessed that approximately satisfies the differential equation and boundary conditions. An iterative process adjusts the function to bring it into close agreement with the true solution.

For some theoretical background on V-cycles in the multigrid method for unwrapping, and other phase unwrapping methods, see Appendix E.

Smoothing

After phase unwrapping and calculation of the B0 fieldmap, (simple) smoothing is applied using a 3×3 convolution kernel:

$$y[r, c] = \sum_{k=0}^{M-1} \sum_{j=0}^{M-1} h[k, j] x[r - k, c - j]$$

[32, p.420].

Via the smoothing filter, the neighbouring values are weighted as much as the current value for computing a new value.

1.10 Collect acquisition parameters

1.10.1 Introduction

In the current version, only three acquisition parameters need to be provided: echo spacing, phase encoding direction and bandwidth in phase encoding direction (BW_{PE}). For short explanations of the terminology, see Appendix D. For directions where to find the acquisition parameters, see section 1.10.3.

Parameter	Common value at 3T
Echo spacing (in ms)	0.53
Bandwidth of EPI image in phase encoding direction (in Hz/Px)	20-60
Phase encoding direction	posterior to anterior (y-axis)

Table 1.1: Required parameters and common values for fieldmap correction

1.10.2 Usage

The menu for the acquisition parameters is shown in figure 1.17. Please note that the values are just example parameters and need to be adjusted according to the acquisition protocol.

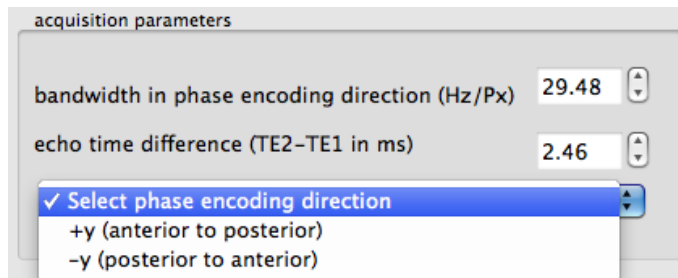


Figure 1.17: Acquisition parameters box

Bandwidth in phase encoding direction

In the 'acquisition parameters' box (see figure 1.17), the bandwidth in the phase encoding direction (BW_{PE}) should be provided³⁴.

For usual scans, this can be computed via: $1 / (\text{echo spacing in seconds} * \text{number of phase encoding lines})$, where the number of phase encoding lines is equal to the matrix size in the phase encoding direction; for example: $1 / (0.53 \text{ msec} * 64 \text{ lines}) = 1 / 0.03392 \text{ sec} = 29.48 \text{ Hz}$. In case the phase encoding is 75%, multiply this with the matrix size of the phase encoding direction. For example: if the image matrix is 128×128 , but the phase resolution is 75%, the bandwidth would become: $1 / (0.53 \text{ msec} * (64 \text{ lines} * 0.75)) = 1 / 0.02544 = 39.31 \text{ Hz}$. The echo spacing and phase resolution can be found on the EPI scan protocol (see figure 1.19).

To calculate the bandwidth, see the conversion utility in section 1.16.3.

³Please note that sometimes the 'echo spacing' is called 'dwell time'. This is the dwell time for the ky dimension [4, p. 716]; but usually the word 'dwell time' is used as time between successive samples in the kx dimension [4, p.367]. See also figure 1.18.

⁴Please note that the bandwidth mentioned on the Siemens scan protocols is bandwidth in the read out direction, not the phase encoding direction.

Echo time difference

Then, enter the difference in echo time in milliseconds between the original phase images, also called the (*phase*) *evolution time*. For Siemens `gre_field_mapping`, this is default $TE_2 - TE_1 = 7.57 - 5.11 = 2.46$ ms (see the `gre_field_mapping` protocol in figure 1.20).

Phase encoding direction

Also, information about the phase encoding direction of the EPI images is required. This information can be derived from the scan protocols (see figure 1.19) or scanner console. Since the first gradient, the readout, is usually in the x-direction, the second gradient, the phase encoding, is usually in the y-direction.

The coordinate system in the scanner is usually the DICOM coordinate system: x: right → left, y: anterior → posterior, z: inferior → superior (see Appendix, section B).

1.10.3 Background

Finding the phase encoding direction, echo spacing and bandwidth of the EPI images

When the pulse has been applied, all signals coming from the spinning H_0 protons in the head would have about the same frequency: the Larmor frequency 42.5MHz multiplied with the strength of magnetic field (for example 3 Tesla). To distinguish between signal at different locations of the brain, the signal is modulated. For the read-out direction (X), the frequency of the signal is modified; this is called *frequency encoding*. For the Y direction, the phase of the signal is modified; this is called *phase encoding*. This makes it possible for each of the 64×64 points in a slice to be uniquely identified: it has its own frequency and its own phase (see figure 1.18).

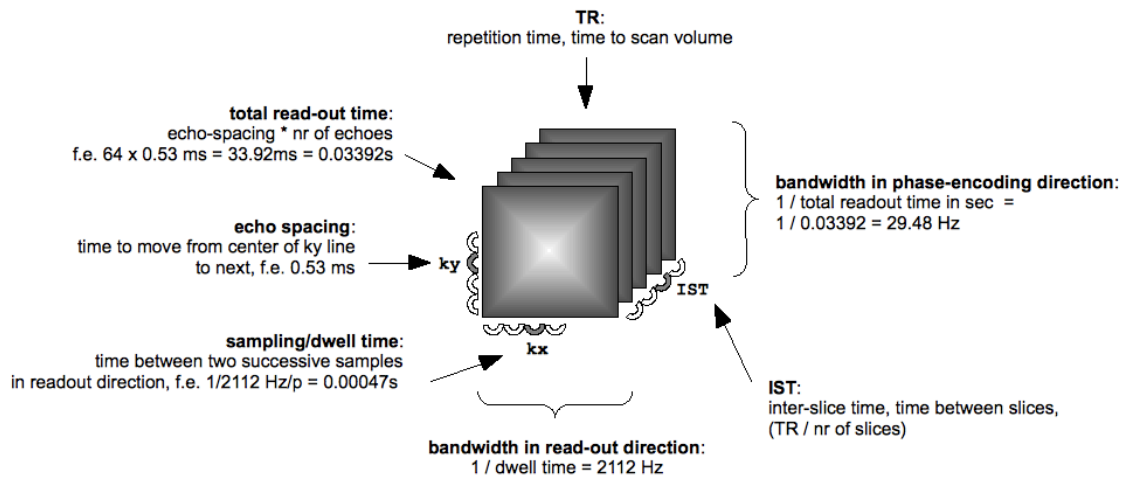


Figure 1.18: Parameters that are relevant for echo-planar imaging: bandwidths in phase and frequency direction, total read-out time, dwell time.

The phase encoding direction and echo spacing can also be found on the acquisition protocol (see figure 1.19)⁵.

⁵The bandwidth that is mentioned on the EPI scan protocol is not the bandwidth in phase encoding direction, but in the read direction.

SIEMENS MAGNETOM Allegra syngo MR A30

\\USER\		
Scan Time: 5:06 Voxel size: 2.0x2.0x2.5 [mm] Rel. SNR: 1.00 USER: ep2d_bold_noprep		
Routine		
Slice group 1		
Slices	21	
Dist. factor	0 [%]	
Position	Isocenter	
Orientation	Transversal	
3 Phase enc. dir.	A >> P	
Rotation	0 [deg]	
Phase oversampling	0 [%]	
FoV read	256 [mm]	
FoV phase	75.0 [%]	
Slice thickness	2.5 [mm]	
TR	1250 [ms]	
TE	25 [ms]	
Averages	1	
Concatenations	1	
Filter	None	
Coil elements	HE	
Adjust volume		
Position	Isocenter	
Orientation	Transversal	
Rotation	0 [deg]	
R >> L	256 [mm]	
A >> P	192 [mm]	
F >> H	53 [mm]	
Physio		
1st Signal/Mode	None	
BOLD		
t-Test	0	
Threshold	4.00	
Window	Growing	
Dynamic t-maps	0	
Starting ignore meas	0	
Paradigm size	20	
Meas[1]	Ignore	
Meas[2]	Ignore	
Meas[3]	Baseline	
Meas[4]	Baseline	
Meas[5]	Baseline	
Meas[6]	Baseline	
Meas[7]	Baseline	
Meas[8]	Baseline	
Meas[9]	Baseline	
Meas[10]	Baseline	
Meas[11]	Ignore	
Meas[12]	Ignore	
Meas[13]	Active	
Meas[14]	Active	
Meas[15]	Active	
Meas[16]	Active	
Meas[17]	Active	
Meas[18]	Active	
Meas[19]	Active	
Meas[20]	Active	
Motion correction	0	
Spatial filter	0	
Sequence		
Introduction	0	
Bandwidth	2790 [Hz/Px]	
Free echo spacing	0	
1 Echo spacing	0.42 [ms]	
EPI factor	96	
Contrast		
MTC	0	
Flip angle	90 [deg]	
Fat suppr.	Fat sat.	

Averaging mode	Long term	
Reconstruction	Magnitude	
Measurements	245	
Delay in TR	0 [ms]	
Multiple series	0	
Resolution		
Base resolution	128	
2 Phase resolution	100 [%]	
Phase partial Fourier	Off	
Filter 1		
Raw filter	Off	
Filter 2		
Large FoV	Off	
Filter 3		
Normalize	Off	
Filter 4		
Elliptical filter	Off	
Trajectory	Cartesian	
Interpolation	0	

PAT mode	None	
Geometry		

Figure 1.19: Acquisition parameter protocol for EPI images (Siemens): 1) phase encoding direction 2) phase resolution 3) echo spacing

Finding the difference in echo time (evolution time)

The differential phase map that one can be obtained via the Siemens `gre_field_mapping` sequence (see printed protocol in figure 1.20) is a result of two phase images with different TEs. For the Siemens `gre_field_mapping` sequence, care has been taken that the evolution time, the echo time difference is small enough not to cause wrapping in the phase data (for information about unwrapping, see section 1.9). In the example protocol depicted in figure 1.20 is shown that the first echo time (TE1) is 5.11 and the second echo time (TE2) is 7.57, so the evolution time is $7.57 - 5.11 = 2.46\text{ms}$ (0.00246 seconds in SI units).

SIEMENS MAGNETOM Allegra syngo MR A30

\\USER\		\gre_field_mapping	
Scan Time: 1:33	Voxel size: 3.5x3.5x3.5 [mm]	Rel. SNR: 1.00	SIEMENS: gre_field_mapping
Routine Slice group 1 Slices 32 Dist. factor 0 [%] Position L0.7 P15.9 H23.1 [mm] Orientation T > C-14.0 Phase enc. dir. A >> P Rotation 0 [deg] Phase oversampling 0 [%] FoV read 224 [mm] FoV phase 100.0 [%] Slice thickness 3.5 [mm] TR 704 [ms] TE[1] 5.11 [ms] TE[2] 7.57 [ms] Averages 1		Adjust volume ! Position L0.7 P20.2 H22.4 [mm] ! Orientation T > C-14.0 ! Rotation 0 [deg] ! R >> L 144 [mm] ! A >> P 194 [mm] ! F >> H 112 [mm]	
		Sequence Introduction 1 Dimension 2D Asymmetric echo Off Contrasts 2 Bandwidth 260 [Hz/Px] Flow comp. Yes ----- RF pulse type Normal Gradient mode Normal	

Figure 1.20: Acquisition parameter protocol for phase fieldmap images (Siemens):
1) echo time 1 and echo time 2

1.11 Coregistration

1.11.1 Introduction

In case the fieldmap have different measurement parameters (orientation, number of slices, etc) than the EPI data, the 'Coregistration' option can be used. This will map the pixelshift image to the space of the EPI data.

1.11.2 Usage

The menu for the acquisition parameters is shown in figure 1.17. Please note that the values are just example parameters and need to be adjusted according to the acquisition protocol.

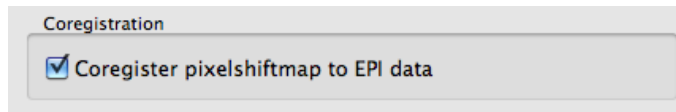


Figure 1.21: Coregistration option for fieldmap to EPI data mapping

1.11.3 Background

The code from the fmr2vmrplugin is used to calculate the new coordinates for the pixelshiftmap. This code is inspired by the initial alignment procedure in Brain-Voyager. In the fmr2vmrplugin and anatabacus, the VMR is used to achieve a FMR > FMR mapping.

1.12 Creating a field inhomogeneity map

In this section is described how to create a field inhomogeneity map of the static magnetic field B_0 .

1.12.1 Usage

Enter the acquisition parameters. Click the button “Proceed to file upload”. Select a filetype. Load the field inhomogeneity map (`*_unwrapped.fmr`) via the “get field inhomogeneity map” button on the dialog (see figure 1.22)⁶.

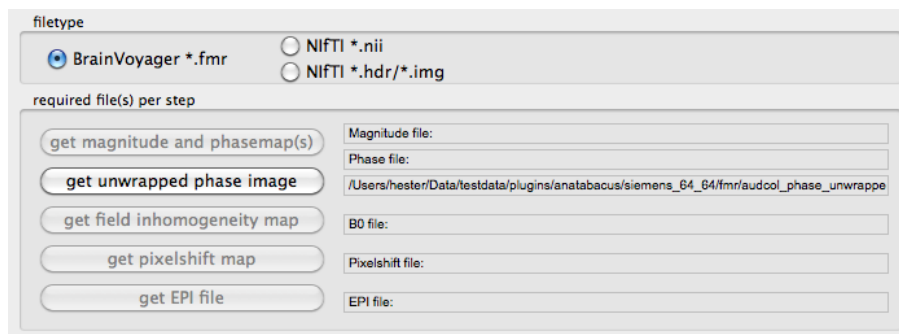


Figure 1.22: Button for selecting unwrapped file

Then, click “Start processing”.

The values in the phase map are converted from radians to Hertz ([29, Ch.12], see figure 1.49). Then, the echo time difference is used to compute to field inhomogeneity for each voxel.

As a result, a field inhomogeneity map `*_b0.*` in BrainVoyager `*.fmr` and `*.amr` will be available. If the B_0 inhomogeneity map appears dark, change the display via BrainVoyager’s Options menu → Contrast and Brightness... (see figure 1.23).

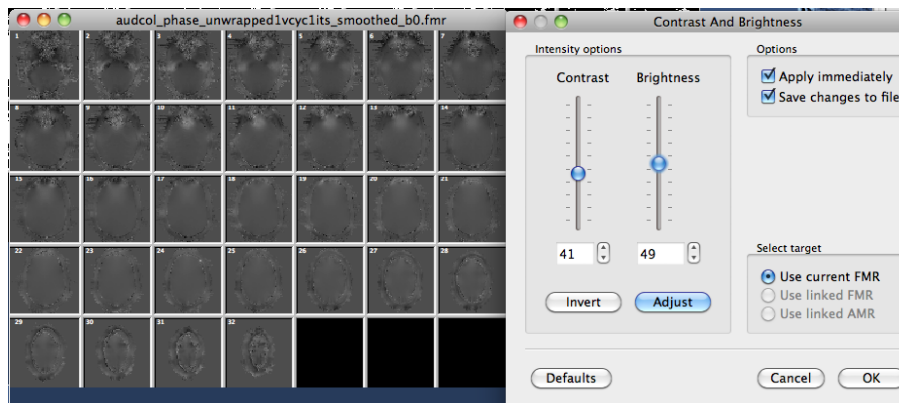


Figure 1.23: Field inhomogeneity map

⁶in this first version: to use a *.nii image: load an *.fmr image in BrainVoyager with the same dimensions

1.12.2 Background

According to Jezzard & Balaban [22], the field inhomogeneity can be computed from the field phase map using:

$$\Delta B_0(x, y, z) = (2\pi\gamma\Delta TE)^{-1}\Delta\phi(x, y, z). \quad (1.1)$$

The field inhomogeneity map can range from for example -200 Hz to 200 Hz for a 3T scanner (see figure 1.24):

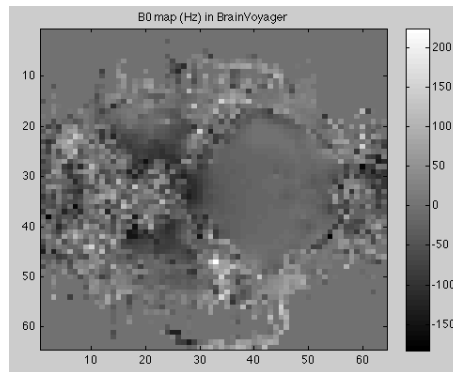


Figure 1.24: Static magnetic field B0 inhomogeneity map computed in BrainVoyager, displayed in Matlab

The conversion from angular frequency ω in radians per second to frequency Hertz f in cycles per second is illustrated in figure 1.49).

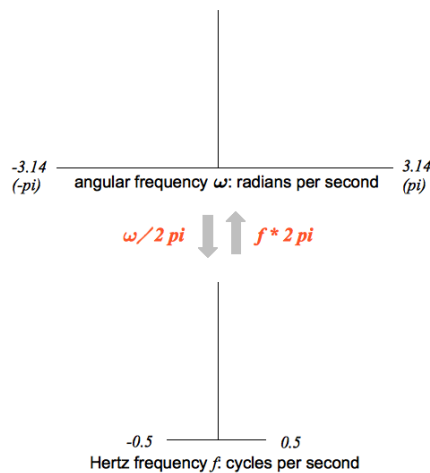


Figure 1.25: Conversion from radians ω to Hertz f : two representations in the frequency (Fourier) domain

1.13 Calculate pixel shift map

The pixel shift map is used to compute how much the pixels have moved because of the local inhomogeneity of the static magnetic field. The pixel shift map is based on the field phase map.

1.13.1 Usage

Enter the acquisition parameters. Click the button “Proceed to file upload”. Select a filetype. Load the field inhomogeneity map (*_b0.fmr) via the “get field inhomogeneity map” button on the dialog. Then, click “Start processing”.

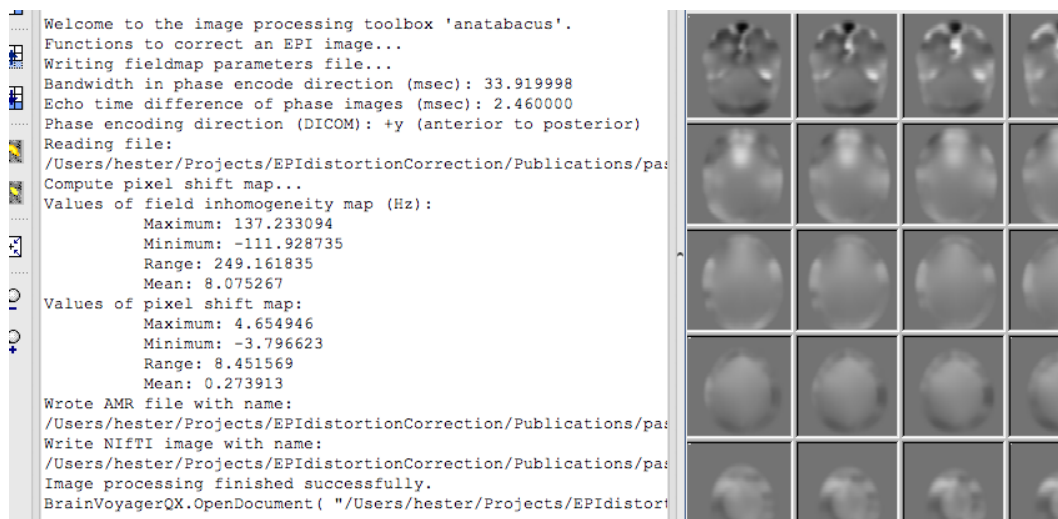


Figure 1.26: Computing a pixelshift map

One pixel shift map is computed per fieldmap (for more information, see section 1.13.2). The pixel shift map is written to disk (*_pixshift.fmr/amr), see figure 1.26). The minimum, maximum and average pixel shift is also printed to the BrainVoyager QX Log tab.

A pixelshiftmap with quantities indicated is shown in figure 1.27.

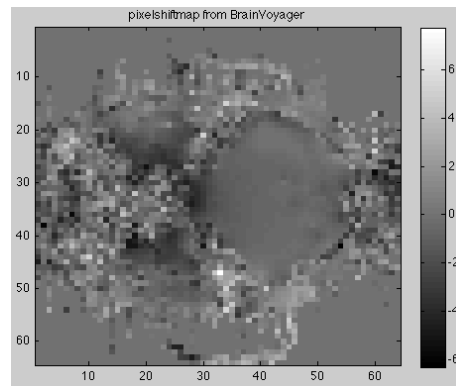


Figure 1.27: A pixelshift map computed in BrainVoyager, displayed in Matlab with quantities

1.13.2 Background

The shift in pixels is determined according to Jezzard & Balaban [22, p.68] by:

The phase encode shift, in units of pixels, is equal to the measured field inhomogeneity, converted to Hz, and divided by the effective spectral width per pixel.

Or in mathematical form:

$$\Delta r_{pe} = \gamma \Delta B_0(x, y, z) \cdot N(2\tau_{ramp} + N \cdot DW)$$

where γ is the gyromagnetic for water protons 1H , $\Delta B_0(x, y, z)$ is the static magnetic field deviation in Hertz for a specific field strength, N is the matrix size ($N \times N$), τ_{ramp} = the ramp time of the switched gradients (in [22] gradient ramp time of 200μ seconds on a 1.5T scanner).

The resulting pixelshift is only calculated in the phase encoding direction, which is usually along the y-axis (in the DICOM coordinate system, see figure B.1).

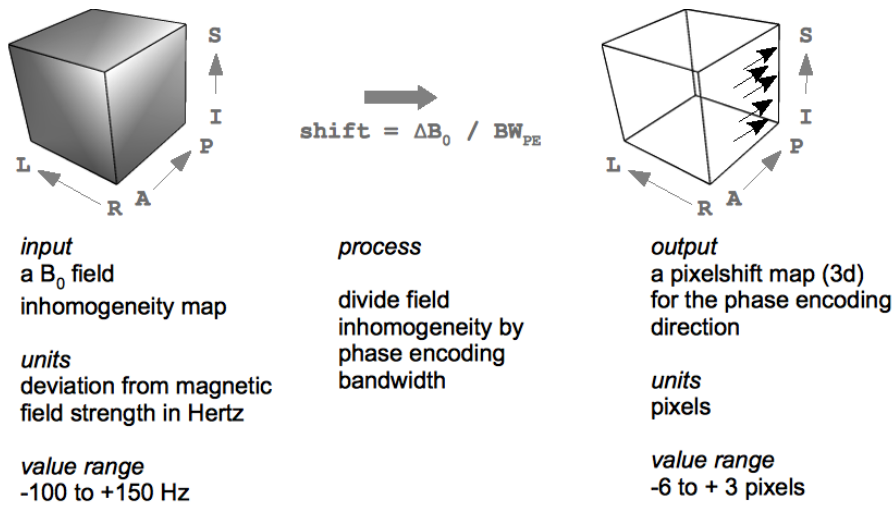


Figure 1.28: Creating a pixelshift map (value ranges adopted from Jezzard & Balaban's article)

1.14 Undistort functional data with pixel shift map

With this function, the EPI images will be unwarped (undistorted) via 1-dimensional interpolation.

1.14.1 Usage

Load the pixelshift map and the functional image via the GUI of the plugin. Click the “Start processing” button.

The “undistort” option will take the pixelshiftmap and interpolate the distorted image to undistort the EPI image (see figure 1.29).

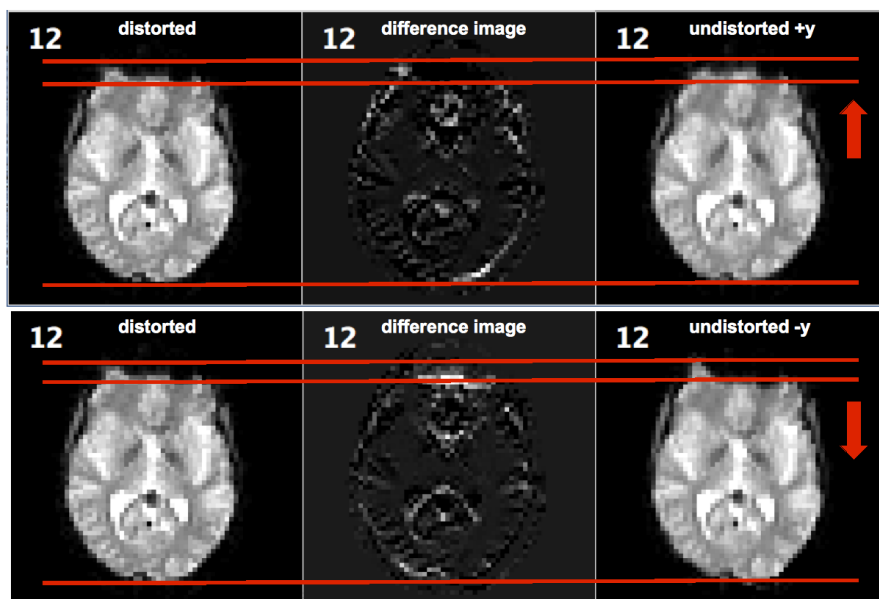


Figure 1.29: Result of undistortion by unknown phase encoding direction; we tried +y and -y: +y seems the proper direction.

As a result of the unwarping process, the coregistration between the functional and anatomical data should be easier, because the unwarped functional data should be closer to their true position.

The difference between the distorted and undistorted image can be visually inspected by subtracting the two FMR projects from each other via the “Evaluation” tool (see section 1.15). (Please note that the effect is only visible after detaching the original AMR.)

See also figure ?? for illustrations of different undistortion results due to various settings. Please note that trying different settings is encouraged, because the optimal settings could differ for each dataset.

Coregistration (“Initial Alignment”) and resampling of pixelshift map

If the fieldmap has been acquired in the same scanning session, but with a different orientation and/or resolution and/or number of slices, the transformation can be calculated and applied to the pixelshift map, so that values from the proper position in the pixelshift map are used to correct the EPI data.

The procedure is as follows.

At first, the plugin will check whether the images are in the same space by comparing the direction vectors.⁷

Resampling

If the pixelshift map has a different size as the functional data, a question dialog will appear to ask whether the orientation of the slices and the Field of View (FOV: image matrix size \times pixel size) of the two dataset are similar (see figure 1.30). If this is the case, the pixelshift map will be resampled using the affine transformation code by Thevenaz (2000, [35]).

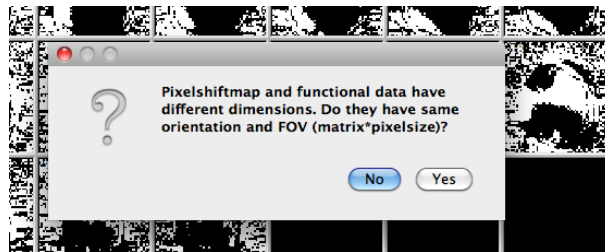


Figure 1.30: Question dialog asking whether resampling is possible

⁷Comparison by taking scalar product of coordinate vectors of the fieldmap in one dimension multiplied by the transpose of the coordinate vector of the EPI image in the same dimension, this should be 1 in case the space is similar; this should be done for all three (x, y, z) directions.

1.14.2 Extent of the distortion

The maximum, minimum and mean pixelshift is always printed to the BrainVoyager QX Log tab when applying undistortion (see figure 1.31). Besides the difference image, which will provide a visual impression of the pixelshift (see section 1.15), these values will provide an impression of the pixelshift in numbers.

```
Undistort in direction: +y (anterior to posterior)
Values of pixelshift data in undistort1d:
Maximum: 5.730897
Minimum: -6.406825
Range: 12.137722
Mean: -0.023150
```

Figure 1.31: The pixelshift values of a particular dataset from a 3T scanner, printed to the BrainVoyager QX Log tab

Concerning the extent of the distortion, hence the pixelshift, see the excellent fieldmap-based EPI distortion correction review of Hutton et al (2001, [18]) and the elaborate group-based review by Cusack et al (2003, [8]). The shift for regions of interest (ROIs) before and after distortion correction has been quantified for a few subjects on volume and surface (see Breman et al, 2010 [5]). A figure of this publication has been reproduced below (see figure 1.32). For a quantification of the distortion at 3T for datasets of individuals, please see the poster of [5], which can be downloaded from Breman et al (2010b) PDF.

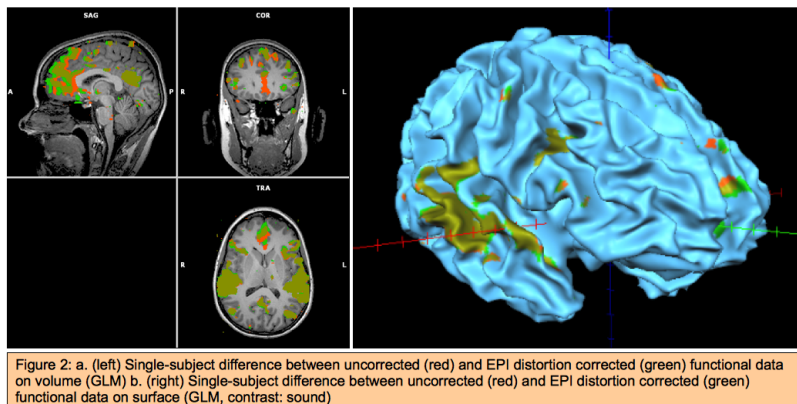


Figure 1.32: Figure of shift of ROIs on volume and surface

1.14.3 Background

The intensity value of each pixel is recalculated by taking into account the distorted grid, using the pixelshift map (see figure 1.33).

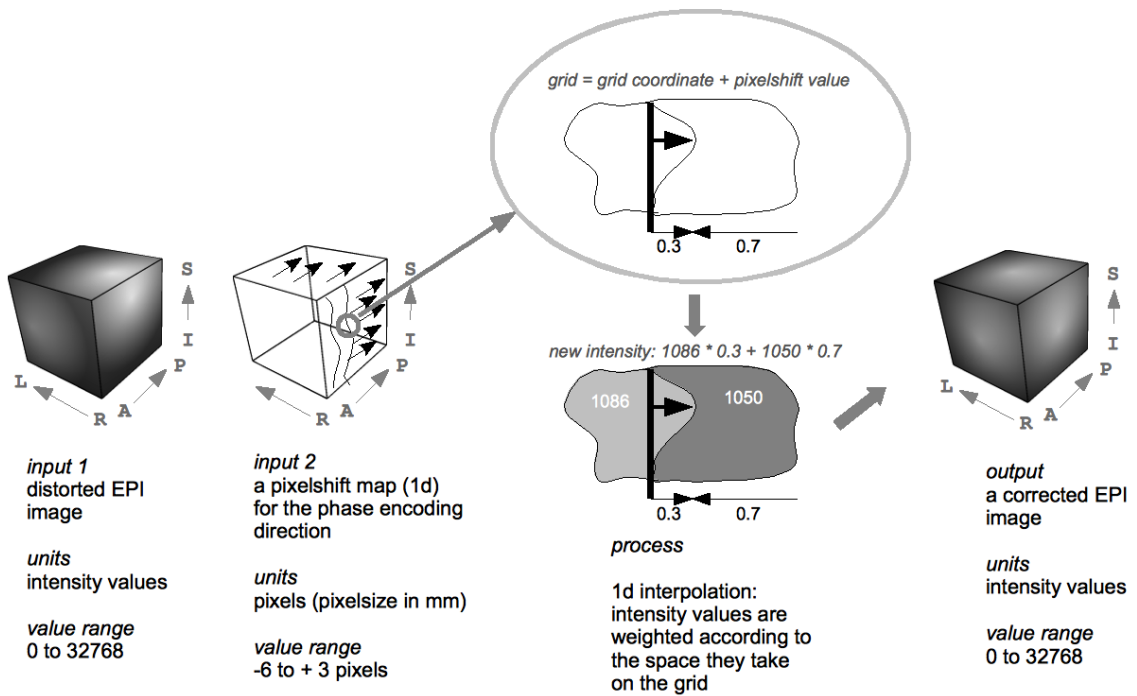


Figure 1.33: The intensity value of each pixel is recalculated by taking into account the distorted grid, using the pixelshift map

1.15 Evaluation utility (create difference image)

With the “Evaluate” function, the distorted and undistorted EPI images can be compared (it is actually possible to compare any two FMR projects with the same number of voxels) by creating a difference image.

1.15.1 Usage

Load the distorted file by clicking the “Get distorted EPI image” button. Then, load the undistorted/unwarped file via the “Get undistorted EPI image” button. The two images will be opened in the BrainVoyager QX window by the plugin. To create a difference image, click the “Create difference image” button (see figure 1.34). This makes it possible to select the source image and the image that should be subtracted (the first image does not necessarily need to be the distorted one and the second the undistorted; in fact, if the distorted is subtracted from the undistorted, the white pixels tell which voxels are ‘new’). The difference image will also become visible in the BrainVoyager QX window (see figure 1.35).

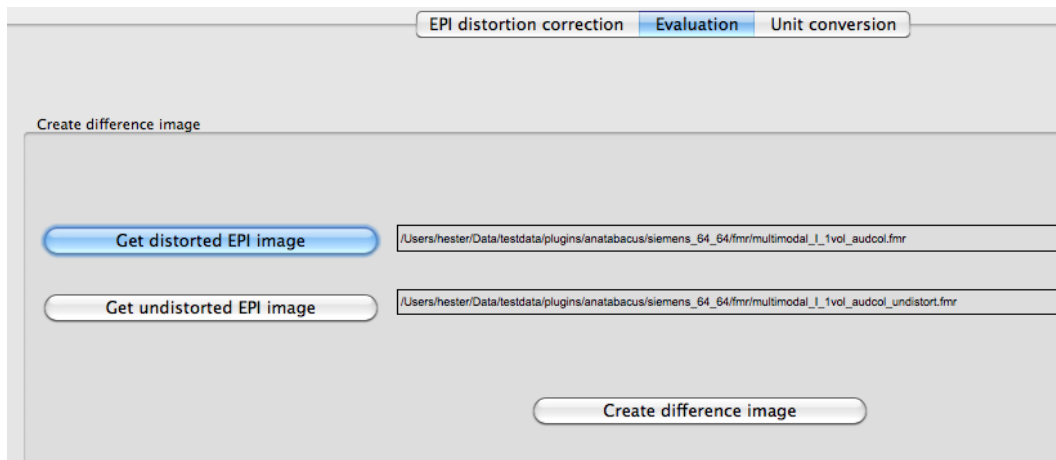


Figure 1.34: Evaluation tab of anatabacus dialog

The image will be saved in the directory of the subtracted image. Please note that the effect of the undistortion is only visible after detaching the original AMR.

Other usage

Remark: with the “Evaluate” function, it is possible to subtract any FMR datasets from each other, not necessarily distortion correction-related datasets. However, please note that the dimensions of the two datasets (number of rows, number of columns, number of slices and number of volumes) should be the same.

An example of other use is the subtraction of two phase images which represent the first and second echo. This creates a differential phase image containing the “phase evolution” between the two echos, which can be used to calculate a map of the static magnetic field B_0 . In this case, when subtracting phase images, they both should be in the same units, for example radians (between $-\pi$ and π).

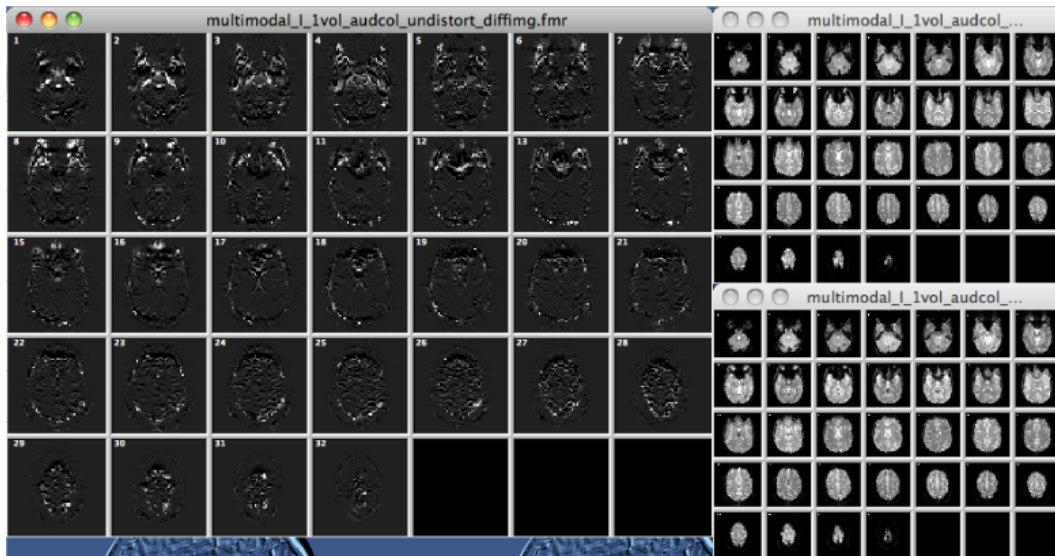


Figure 1.35: Difference image (large) and distorted and undistorted FMR images

1.15.2 Evaluation via coregistration with anatomy

A simple way to check what the effect of the distortion correction is, and to evaluate whether it was performed in the proper direction (+y or -y), is to compare the initial alignment between functional and anatomical data before and after distortion correction.

To perform this, open the untransformed anatomical image that was acquired during the same experiment. Then, via the Coregistration tab of the 3D Volume Tools, select the distorted functional image (*.fmr) and click the “Run IA” button (IA: initial alignment). Then, open another copy of the untransformed anatomical image and run initial alignment with the undistorted functional image. The undistorted functional image should fit better on the anatomical image (see figures 1.36 and 1.37).

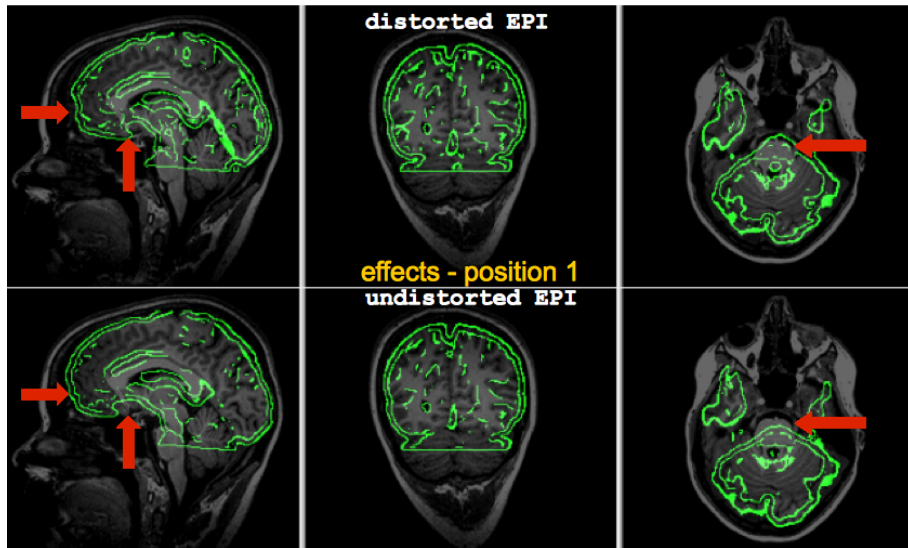


Figure 1.36: Visualisation of effects of the distortion correction at position 1 (inferior cross position). *Top figure:* Coregistration (initial alignment) with distorted EPI. *Bottom figure:* Coregistration (initial alignment) with corrected EPI; anteriorly the brain has expanded due to positive pixelshifts, while in the middle compression is visible due to negative pixelshift.

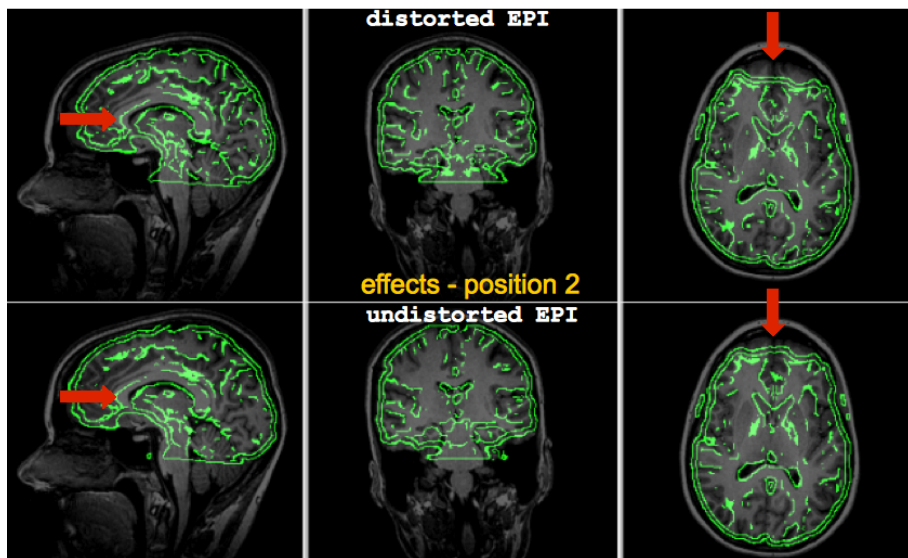


Figure 1.37: Visualisation of effects of the distortion correction at position 2 (more superior cross position) *Top figure:* Coregistration (initial alignment) with distorted EPI. *Bottom figure:* Coregistration (initial alignment) with corrected EPI. The functional image fits now better on the corpus callosum; anteriorly, the functional image is stretched.

1.16 Conversion utilities

The conversion utilities can be found on anatabacus' conversion tab (see figure 1.38).

The screenshot shows the 'Unit conversion' tab in the anatabacus software. The interface is divided into several sections:

- Convert to (derived) SI units:** This section contains four rows of input fields. The first row has 'amount: 42.5'. The second row has 'time' and 'seconds' with a 'select quantity' dropdown. The third row has 'position' and 'meters' with a 'select quantity' dropdown. The fourth row has 'frequency' and 'hertz' with a 'megahertz' dropdown and the value '42500000'. A 'convert' button is at the bottom right of this section.
- Other calculations:** This section has a list of radio buttons: 'degrees to radians' (selected), 'radians to degrees', 'radians to hertz', 'ppm to hertz', 'echo spacing to phase encoding bandwidth', and 'frequency shift to pixel shift'. To the right are three input fields with values '180.0000000000', '0.0000000000', and '0.0000000000'. A 'radians: 3.141592654' field is also present. A 'convert' button is at the bottom right.
- Convert Cartesian to polar coordinates:** This section has 'real' and 'imaginary' input fields with values '2' and '1'. 'magnitude' and 'phase' output fields show '2.2361' and '0.4636'. A tooltip 'Convert real and imaginary to magnitude and phase' is visible over the conversion arrows. A 'convert' button is at the bottom right.
- Convert Cartesian to polar coordinate files:** This section has 'get real file' and 'get imaginary file' buttons. A 'convert files to polar' button is at the bottom right.

Figure 1.38: anatabacus' conversion tab

1.16.1 Conversions: to SI units

Convert time

It is possible to convert to seconds (figure 1.39) from the quantities mentioned in table 1.16.1.

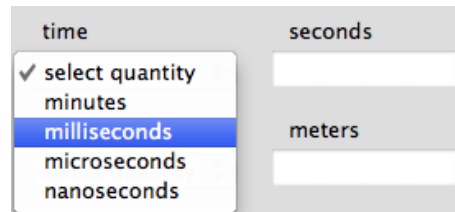


Figure 1.39: Convert to SI unit in time

<i>quantity to</i>	<i>seconds</i>
minutes (min)	$\times 60$
milliseconds (msec)	$\times 10^{-3}$
microseconds (μs)	$\times 10^{-6}$
nanoseconds (ns)	$\times 10^{-9}$

Table 1.2: Conversion of time to SI unit 'seconds'

Convert position

Convert distances listed in table 1.16.1 via the position utility (figure 1.40).

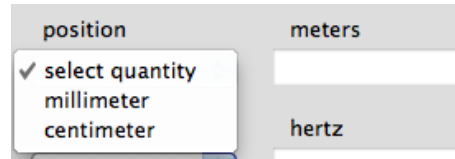


Figure 1.40: Convert to SI unit in position

<i>quantity to</i>	<i>meters</i>
millimeters	$\times 10^{-3}$
centimeters	/ 100

Table 1.3: Conversion of position to SI unit 'meter'

Convert frequency

For conversion of frequencies to SI unit 'hertz', there is a conversion option as well (figure 1.41). The possibilities are listed in table 1.16.1.

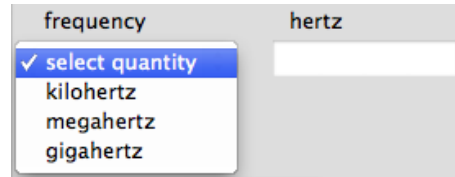


Figure 1.41: Convert to SI unit in frequency

<i>quantity to</i>	<i>hertz</i>
kilohertz (KHz)	$\times 10^3$
megahertz (MHz)	$\times 10^6$
gigahertz (GHz)	$\times 10^9$

Table 1.4: Conversion of frequency to SI unit 'hertz'

1.16.2 Conversions: between Cartesian and polar coordinates

Complex numbers, like the signal acquired from the scanner (magnitude and phase images), can be expressed in real and imaginary coordinates or magnitude and phase. To convert between the two representations, the utility depicted in 1.42 can be used.

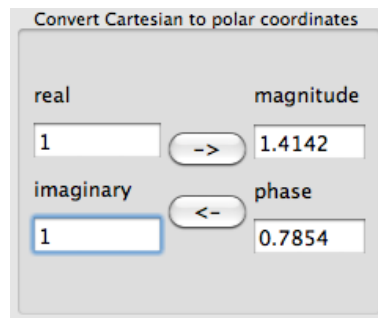


Figure 1.42: Convert between Cartesian and polar coordinates

Cartesian coordinates (real and imaginary) to polar

To convert from Cartesian coordinates $z = x + iy$ to the polar form $z = re^{i\theta}$, fill the 'real' and 'imaginary' text fields and click the button with the arrow to the right ' \rightarrow ': see figure 1.43. Magnitude r is calculated via $r = \sqrt{x^2 + y^2}$. Phase θ is calculated using the arctangent: $\theta = \tan^{-1}(\frac{y}{x})$.⁸

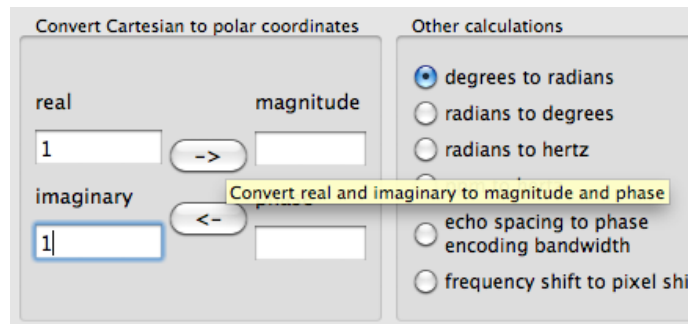


Figure 1.43: Convert Cartesian to polar coordinates

⁸Magnitude and phase are sometimes also called *modulus* and *argument*.

Convert rectangular/cartesian to polar files

Sometimes real and imaginary fieldmaps are available rather than phase and magnitude fieldmaps (see figure 1.44).

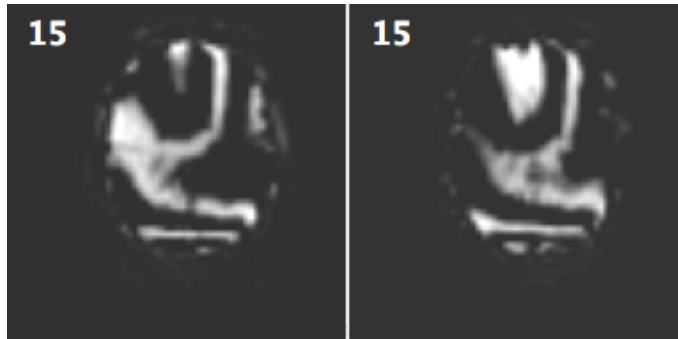


Figure 1.44: Real (left) and imaginary (right) fieldmap slices

For these cases, the “Convert rectangular to polar” option can be applied (see figure 1.45). This will then convert the real and imaginary data to magnitude and phase images. This is required for the distortion correction procedure.

Note October 2011: Until further notice, it is recommended to do the conversion outside BrainVoyager since the negative values in the real and imaginary data will be truncated to zero when creating an FMR project, which will provide incomplete phase data which cannot be unwrapped properly.

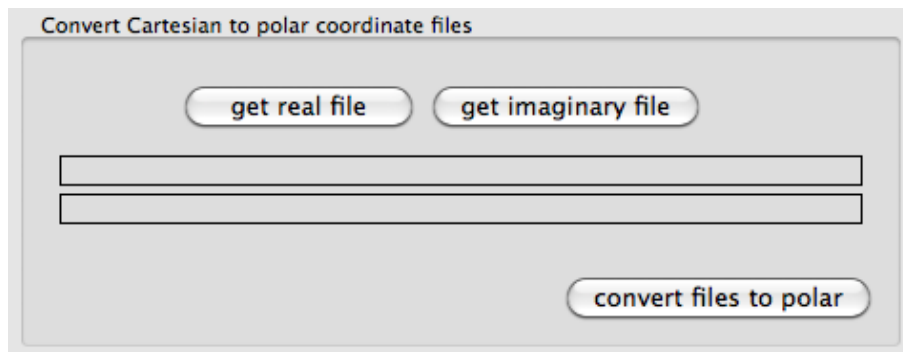


Figure 1.45: Convert Cartesian to polar coordinates

Polar coordinates (magnitude and phase) to Cartesian (real and imaginary)

To convert from polar coordinates $z = re^{i\theta}$ to Cartesian form $z = x + iy$, fill the 'magnitude' and 'phase' text fields and click the button with the arrow to the left ' \leftarrow ': see figure 1.46. Conversion is computed using Euler's formula $re^{i\theta} = r(\cos \theta + i \sin \theta)$ [31, Ch.3]. Note that the phase should be entered in radians. For conversion from degrees to radians, the conversion utility for degrees to radians as described in section 1.16.3 can be applied.

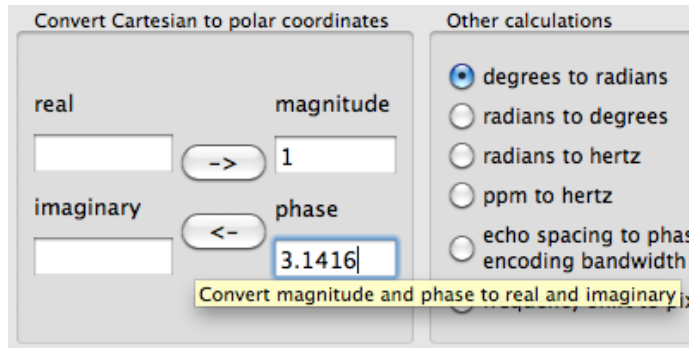


Figure 1.46: Convert Cartesian to polar coordinates

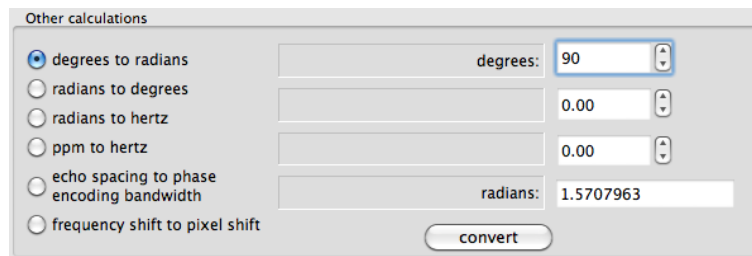
1.16.3 Conversions: other calculations

Degrees to radians

Description: Convert an angle in degrees (0-360) to an angle in radians (0- 2π).

Input: degrees

Output: radians



The screenshot shows a dialog box titled "Other calculations" with several radio button options. The "degrees to radians" option is selected. The "degrees:" input field contains the value "90". The "radians:" output field displays the result "1.5707963". A "convert" button is located at the bottom right of the dialog.

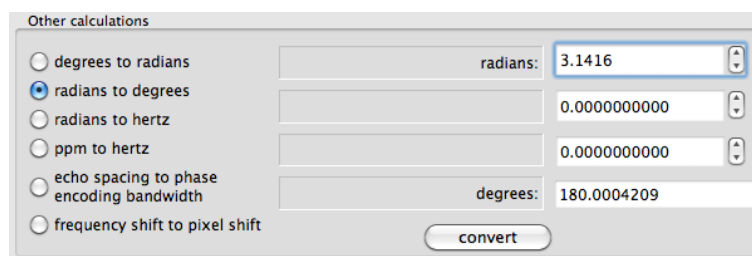
Figure 1.47: Convert degrees to radians

Radians to degrees

Description: Convert an angle in radians (0- 2π) to an angle in degrees (0-360).

Input: radians

Output: degrees



The screenshot shows the same "Other calculations" dialog box, but now the "radians to degrees" option is selected. The "radians:" input field contains the value "3.1416". The "degrees:" output field displays the result "180.0004209". The "convert" button remains at the bottom right.

Figure 1.48: Convert radians to degrees

Radians to hertz

Description: This is a function to convert angular frequency ω (in radians per second) to frequency f in hertz (in cycles per second) according to $\omega = 2\pi f$ and $d\omega = 2\pi d f$ (see Bernstein et al; [4, p.9]).

Input: radians

Output: hertz

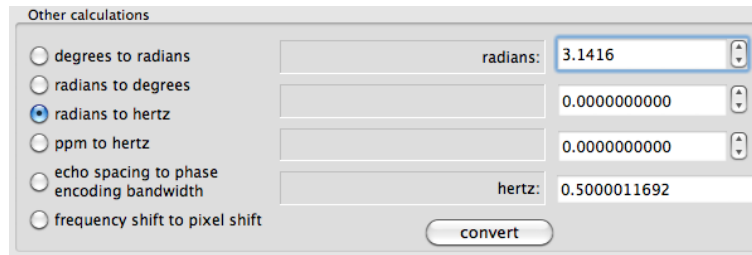


Figure 1.49: Convert radians to hertz

Parts-per-million to hertz

Description: This is a function to convert static magnetic field inhomogeneity in parts-per-million (ppm) to hertz (Hz), when using fieldmaps created in other software packages, for example FUGUE in FSL. This assumes a resonance frequency of 42,576,000 Hz (for water protons 1H).

Input 1: parts per million (ppm)

Input 2: static magnetic field strength B_0 in Tesla (T)

Output: static magnetic field deviation ΔB_0 in hertz (Hz)

The conversion is $\text{ppm} \times (\text{resonance frequency} \times B_0) = \Delta B_0$ in hertz (Hz).

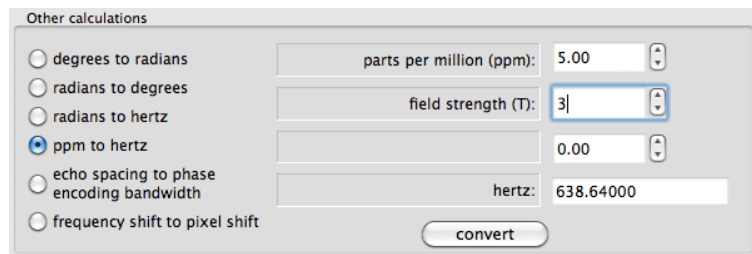


Figure 1.50: Convert parts-per-million to hertz

Echo spacing to phase encoding bandwidth

Description: One of the required acquisition parameters is 'bandwidth in phase encoding direction (Hz/Px)'. The current function can be used to compute this value.

Input 1: echospacing in milliseconds, for example 0.53

Input 2: number of phase encoding lines (rows in image), for example 64

Input 3: SENSE/GRAPPA acceleration factor; default: 1

Output: bandwidth in phase encoding direction (Hz)

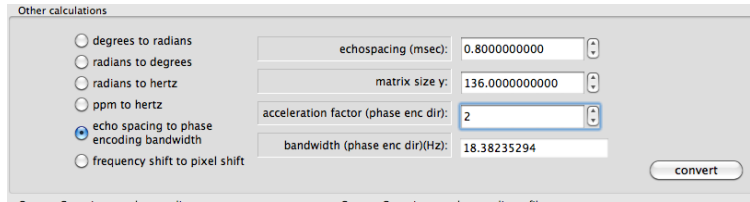


Figure 1.51: Convert echo spacing to phase encoding bandwidth

Field inhomogeneity to pixel shift

Description: This is a function to compute the pixel shift from the static magnetic field B_0 deviation in Hz, like in the distortion correction procedure. Basis is the *Fourier shift theorem*, which says that a shift or offset of the coordinate in one domain results in a multiplication of the signal by a linear phase ramp in the other domain, and vice versa⁹. [4, p.10]

Input 1: bandwidth in phase encoding direction, for example 28 (Hz)

Input 2: B_0 field inhomogeneity, for example 110 (Hz)

Output: pixel shift

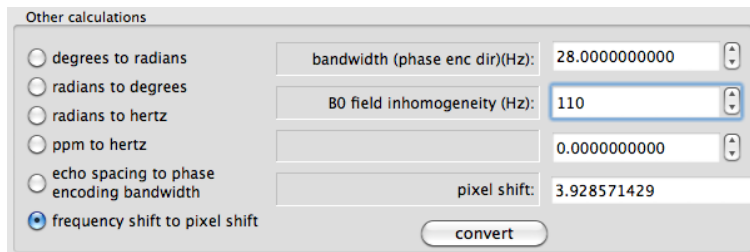


Figure 1.52: Convert field inhomogeneity to pixel shift

⁹Fourier shift theorem: $FT[g(x+a)] = \int_{-\infty}^{\infty} g(x)e^{-2\pi i k(x+a)} dx = G(k)e^{-2\pi i k a}$

1.16.4 Background

There are two systems used in engineering/physics, to denote quantities. The first system is the CKS system (Centimeters-Kilos-Seconds). The second system is the Syst eme International (SI).

If units are not specified, people will assume that the units are SI units; this means that if there is a measure of time, one will assume that this temporal quantity is in seconds (and not in milliseconds, microseconds or minutes).

For units directly relevant to MRI, see table 1.16.4 (from [4, p.958]).

Symbol	Meaning
0	0
T_1 (ms or s)	Spin-lattice relaxation time
T_2 (ms or s)	Spin-spin relaxation time
T_2^* (ms or s)	Apparent spin-spin relaxation time
χ	Magnetic susceptibility

Table 1.5: Spin physical properties

Relevant units according to Syst eme International (SI) [23]:

Name	Unit	Symbol	Description
Length	meter (m)	l	
Time	seconds (s)	ϕ	
Angle	radian (rad)	α, β	

Table 1.6: Ground SI-units

Quantity	Symbol	Unit
Angular frequency	ω	rad/s
Phase/difference	ϕ	rad
Frequency	f,v	Hz (= s^{-1})
Wavelength	λ	m
Period	T	s
Rotational frequency	n	s^{-1}
Radius	R,r	m
Time	t	s
Time constant	τ	s

Table 1.7: Derived SI-units

Appendix A

Acquisition of B0 field maps

A.1 Introduction

EPI images are reconstructed from magnitude data. A phase field map is a difference between two images of phase data or *differential phase image*. These phase images can be obtained using a spin-echo (SE) sequence or a gradient-echo (GRE) sequence. For the phase images to be useful, they are first processed to a differential phase image which indicates how fast the phase on each point in space changes. This information about phase changes at each point is then used to compute the displacement of each pixel in the EPI image.

A.2 Phase map types

A.2.1 Spin-echo (SE) phase maps

In case of a spin-echo (SE) sequence, the difference is obtained by the timing of the 180 degrees refocusing pulse, which is for the first image $TE/2$ and for the second image $TE/2 + \tau$. The time difference between these refocusing pulses is called `asymtime` in FSL (see figure D.1). Spin-echo phase maps are much less distorted than gradient-echo phase maps.

A.2.2 Gradient-echo (GRE) phase maps

The phase difference in gradient-echo (GRE) phase maps is obtained by acquiring images at two different echo times. Gradient-echo images are more distorted than spin-echo images because of the reduced signal to noise due to voxel dephasing. Siemens has a double-echo spoiled gradient echo sequence, which is called FLASH (`gre_field_mapping` on the console) which produces a differential phase image (see section A.3.4). Typical echo times in this sequence are 5.11 and 7.57 ms for a 3T scanner and 5.00 and 6.02 ms for a 7T scanner. The second echo time is calculated with respect to the first (see the information in figure ??), and is made as short as possible to reduce wraps in the phase image. This time (here for 3T: 2.46 ms) between the two images is called (*phase evolution time* and notated as δ_{TE}).

A.3 Acquisition of phase field maps

A.3.1 Acquisition on Bruker scanners

On Bruker, one can use the GEFI-TOMO protocol to acquire a pair of gradient echo acquisitions (see Cusack et al [8]).

A.3.2 Acquisition on Philips scanners

On Philips scanners, there seems to be a checkbox labeled “B0” with each scan protocol, which should then provide a map of the static magnetic field B_0 . Also, Philips has a spoiled gradient echo sequence under the name CE-FFE-T1 or T1-FFE [4, p.584]. It is not known whether a double echo can be applied so that a differential phase image can be constructed (any information welcome).

A.3.3 Acquisition on General Electric (GE) scanners

GE has a spoiled gradient echo sequence under the name SPGR [4, p.584]. It is possible to acquire real and imaginary data as fieldmaps. There are also phase and magnitude data, but the phase data might be smoothed, which is not easy to unwrap. Therefore, the real and imaginary data are recommended. For conversion from real and imaginary files to magnitude and phase, see the “Conversion” tab of `anatabacus` described in section 1.16.2.

A.3.4 Acquisition on Siemens Allegra 3T scanner

The acquisition of a gradient-echo field map on the Siemens Allegra is easy to do and takes only about 1 minute. The product is a set of slices that look like the EPI data (magnitude), and a set of slices which consists of a differential phase map. The procedure is the following:

1. Search the `gre_field_mapping` sequence from the Siemens sequences list (see figure A.1).

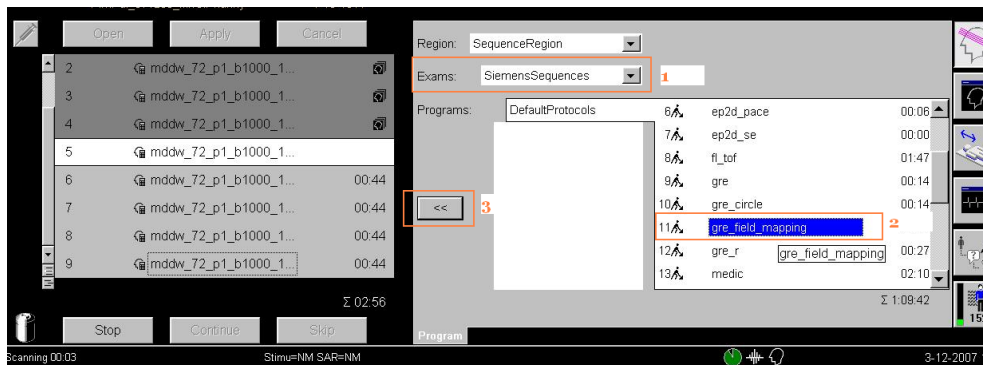


Figure A.1: Adding the Siemens field mapping sequence to the job list: 1. “Exams”, select “SiemensSequences”. 2. In “DefaultProtocols”, select “gre field mapping”. 3. Move the protocol to the joblist

2. Copy the `gre_field_mapping` sequence to the job list (or first to your own user folder); place before the EPI sequence.
3. Copy the positioning information from the EPI sequence to the `gre_field_mapping` sequence. Select the `gre_field_mapping` in the job list and press the “Open” button. Right-click on your EPI data in the job list, and select “Copy measurement parameters”. Do the same for the shimming parameters, by copying the “Adjust Volume” parameters.
4. Make sure that the “Reconstruction” parameter on the “Contrast” → “Dynamic” tab is set to “Magnitude/Phase” (see figure A.2)
5. Run sequences in the job list
6. Export the protocols to PDF because the echo spacing or dwell time is mentioned on the EPI protocol, (see figure 1.19)

The result is two sets of slices, that can be imported as FMR projects in Brain-Voyager (see figure 1.14).

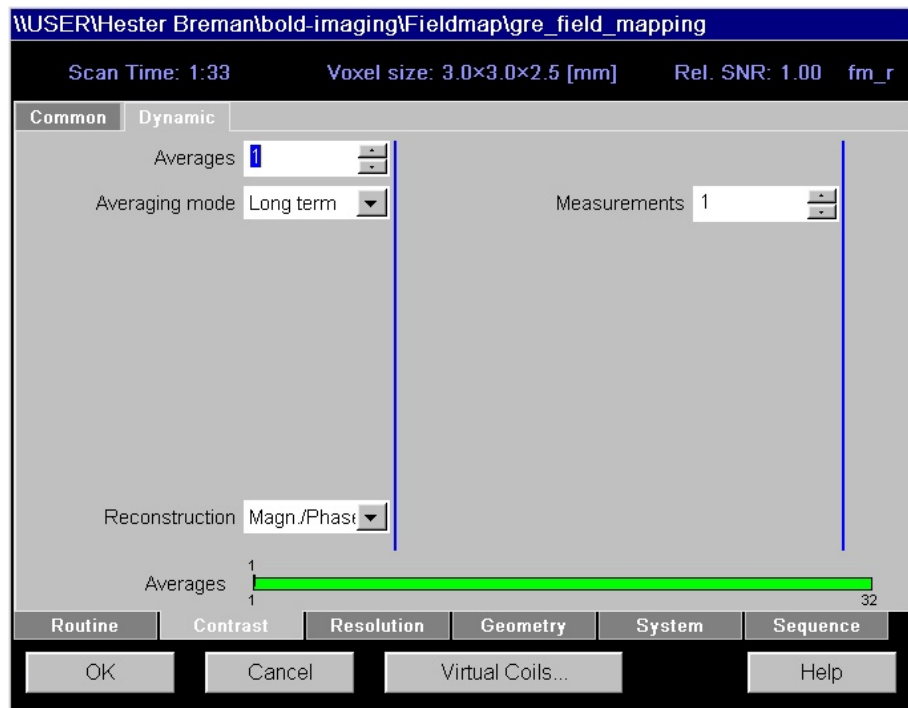


Figure A.2: On the Contrast tab, set the Reconstruction to Magnitude/Phase

A.4 Manually creating a differential phase map from two phase images with different echo times

In case one does not have a standard sequence for acquiring fieldmaps, it should be possible to compute a differential phase map from two similar complex gradient-echo images with different echo times via

$$\Delta\phi = \arctan\left(\frac{\text{Im}(Z_1 Z_2^*)}{\text{Re}(Z_1 Z_2^*)}\right) = \text{ATAN2}[\text{Im}(Z_1 Z_2^*), \text{Re}(Z_1 Z_2^*)] \quad (\text{A.1})$$

where Z_1 is a complex value in phase image 1 and Z_2^* the complex conjugate of a value in phase image 2 (see Bernstein et al [4, par. 13.5.1]).

Alternatively, in case one has two phase images, just subtract the phase image with short echo time (TE1) from the one with long echo time (TE2). For subtraction of FMR images, see section 1.15.

Spin-echo differential phase maps are even superior, in that case two phase images should be acquired with refocusing pulses at different times (see figure D.1).

Appendix B

Summary of coordinate systems in MRI

Because several file formats are used in the fieldmap-based distortion correction part of the *anatabacus* plugin, referring to BrainVoyager, NIfTI and DICOM coordinate systems, these coordinate systems have been depicted in figure B.1.

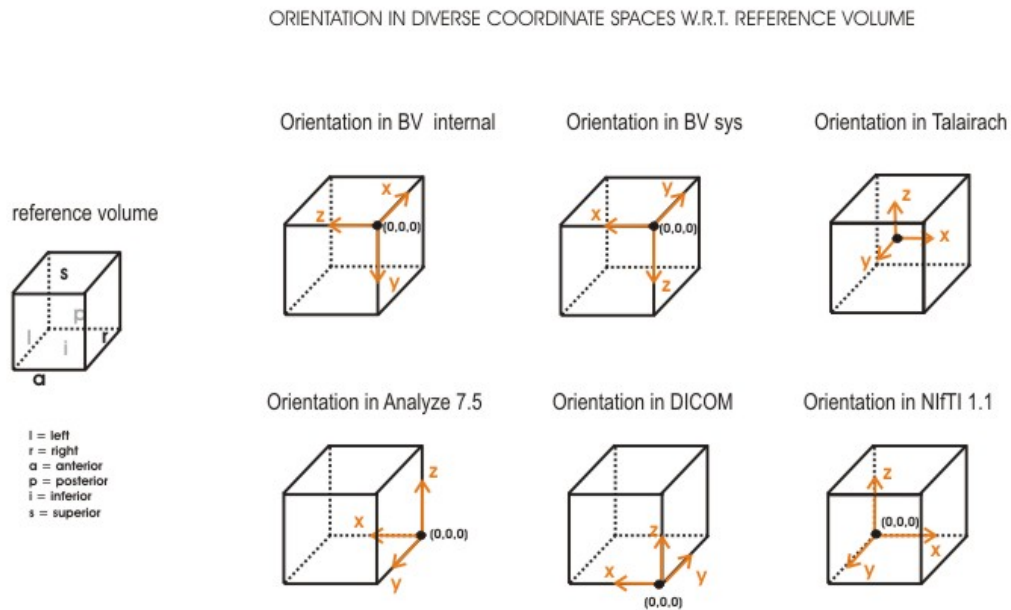


Figure B.1: Coordinate systems in magnetic resonance imaging

B.1 Coordinate systems in Magnetic Resonance Imaging

1. BrainVoyager internal coordinates. Origin at voxel (0, 0, 0).
 X_{BV} : anterior \rightarrow posterior
 Y_{BV} : superior \rightarrow inferior
 Z_{BV} : right \rightarrow left
2. BrainVoyager system coordinates. Origin, directions/values are defined the same as the internal coordinate system but axes names follow Talairach standard:
 X_{SYS} : right \rightarrow left
 Y_{SYS} : anterior \rightarrow posterior
 Z_{SYS} : superior \rightarrow left
3. Talairach coordinates. Axes names like in system coordinates but opposite directions, origin in AC (128,128,128), values defined according to 8 landmarks (AC, PC, LP, RP, SP, IP, AP, PP).
 X_{TAL} : left \rightarrow right
 Y_{TAL} : posterior \rightarrow anterior
 Z_{TAL} : superior \rightarrow left
4. OpenGL coordinates. Like internal (but also shown as BrainVoyager system coordinates to the user, except small axes cross in left lower corner of OpenGL (surface) window.
5. NIFTI 1.1 coordinates
 x : left \rightarrow right
 y : posterior \rightarrow anterior
 z : inferior \rightarrow superior
6. DICOM coordinates
 x : right \rightarrow left
 y : anterior \rightarrow posterior
 z : inferior \rightarrow superior

See also the document about spatial transformation conventions by Jenkinson [21].

Appendix C

Preventive measures

C.1 Reducing susceptibility artifacts

Some measures to reduce susceptibility artifacts are described in the literature. Possible measures are for example a slice tilt, shorter TE, head tilt, passive shimming, dynamic shimming and other k-space trajectories (e.g. spiral) (the last two options require sequence modification).

C.1.1 Global measures

Reducing echo time (TE)

As a global measure, reducing echo time (TE) is an approved method. The echo time (TE) should be reduced as far as possible, but not lower than 25 ms for a 3 Tesla scanner. For effects of TE, please see Gorno-Tempini et al (2002)[16], Weiskopf et al (2006)[36], Stoecker et al (2006)[33] and Hutton et al (2001)[20].

Slice tilt

To reduce signal dropout, see the table for optimal slice positioning in figure C.1a from Weiskopf et al (2006; [36]) and illustration for slice positioning in figure C.1b.

Concerning the direction of the slice tilts, Weiskopf et al state [36]:

Thirdly, slice tilts were limited to less than 45 degrees, because special care must be taken with large slice tilts, in particular positive ones (positive values denote tilts of the anterior edge of the slice towards the feet measured from the axial plane). In this case the slice may intersect with the oral cavity and nose, causing wrap over, chemical shift artifacts (from unsuppressed fatty tissue signals) and larger Nyquist ghost. Therefore, we would recommend using negative slice tilts if possible.

The tilt angle is with respect to the scanner axis. Weiskopf (personal communication) mentioned that

The same slice tilt should be applied irrespective of the head tilt, since 1) the method has been validated using this particular procedure and 2) in our systems (Allegra, Sonata) the intersubject variance in head tilts was relatively small. However, please note that in-between scanners it can be significant due to different coil geometries/scanner couch etc.

Optimal EPI parameters for regions of interest at 3 T

Region of interest	PP [mT/m*ms]	Tilt [deg]	PE	Optimal mean % BS	Standard mean % BS
mOFC+rACC	-1.4	-45	neg.	99.2	83.5
Inferior temporal lobes	-0.4	+30	neg.	78.1	75.1
Temporal poles	+0.6	+30	neg.	106.0	89.5
Amygdala	+0.6	-45	pos.	120.9	107.3
Hippocampus+ Parahippocampus	+0.6	-45	pos.	121.9	109.7

PP=z-shimming prepulse gradient moment; PE=phase-encoding polarity; BS=BOLD sensitivity; mOFC+rACC=medial orbitofrontal cortex and rostral-ventral anterior cingulate cortex with $z < 0$ mm (MNI).

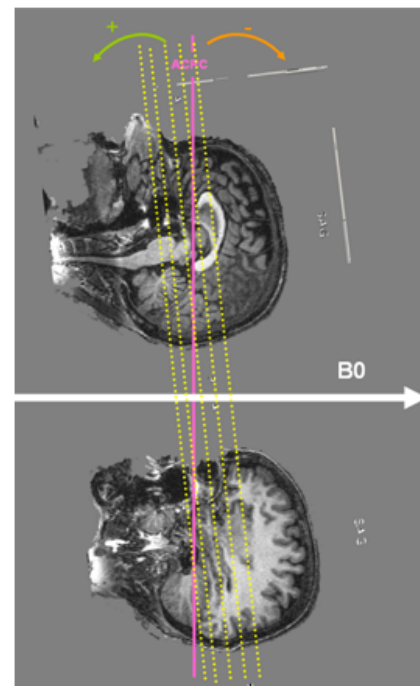


Figure C.1: (a) Table from Weiskopf et al [36]: “For the positive PE polarity, negative slice tilts were optimal in the temporal pole and posterior OFC, and positive slice tilts in the anterior OFC and inferior temporal gyri. In most brain regions, the sign of the optimal slice tilt reversed together with the PE polarity.” (b) Illustration for the table by Valérie Goffaux.

Head tilt

Alternatively, tilting the head is also possible. Heberlein and Hu ([17]) found that a head tilt improves the shim. Barker et al ([2]) also suggests that the head tilt with respect to the direction of the B_0 magnetic field influences the field inhomogeneity. Heberlein and Hu state about the direction of the head tilt:

In the figure a tilt angle of zero degrees means that the AC-PC plane is directly perpendicular to the main magnetic field.

Dreher et al [12] have applied Heberlein and Hu's suggestion:

In addition, we tilted the head of the subject with a 30 angle relative to the AC-PC line because this simple head positioning procedure improves the shim in this area (Heberlein and Hu, 1991).¹

Use different k-space trajectory

Also, some researchers use different trajectories (in particular, spiral sequences) to reduce susceptibility artifacts [14, 24, 34] (the usual scanning trajectory is "cartesian", which means scanning lines in k-space from right to left and vice versa). These sequences have to be developed by MR physicists however, or be acquired from MRI scanner manufacturers.

C.1.2 Region-specific measures

For scanning the temporal lobe or the orbitofrontal cortex, parameters can be adapted to increase the BOLD sensitivity (BS) up to 20% (Weiskopf).

Frontal lobe

To scan the medial frontal lobe, Ojemann et al [28] suggest to use sagittal or coronal orientation with smaller TE.

See also Österbauer et al (2006)[27].

Temporal lobe

See Devlin et al (2000)[11]. See also Bellgowan et al (2006)[3].

Amygdala

For scanning the amygdala, Merboldt et al (2001)[25] observe less distortion when using coronal slice orientation. This is confirmed by Chen et al [7], who state that an optimal selection for the slice orientation is an oblique pseudo-coronal plane

¹Signal dropout in the orbitofrontal cortex due to susceptibility artifact was reduced by using a local high-order z-shimming performed in the axial direction with an oval-shape region that included the orbitofrontal cortex and the basal ganglia. In addition, we tilted the head of the subject with a 30 degrees angle relative to the AC-PC line because this simple head positioning procedure improves the shim in this area (Heberlein and Hu, 1991). Indeed, a region of high field distortion is located above the nasal cavity and a region of low field is located behind the nasal cavity. Since these field effects are dependent on the direction of the main magnetic field relative to the head, it is possible to direct the distortions away from the inferior frontal lobe by using this simple positioning method for acquiring para-axial slices traversing the anterior commissure and the posterior commissure (Heberlein and Hu, 1991). The head position was obtained by slightly increasing the padding on the base of the neck and reducing padding for the back of the head using an air pressure-inflatable pillow. The angle was obtained using a protractor measuring the angle between the vertical and the AC-PC line and was then checked with the sagittal localizer.

with its frequency-encoding direction parallel to the field gradient measured from each subject.
See also Stöcker et al [33].

Shimming

Passive shimming, which also reduces artifacts, is performed by placing diamagnetic objects in subjects' air cavities like the mouth. Wilson et al (2002) use pyrolytic graphite [37]. See also [27]. For an evaluation of passive shimming, see Cusack et al (2005)[10].

Most other shimming measures (e.g. z-shimming) require sequence modification.

Appendix D

Nomenclature

D.1 Nomenclature

Please find below a glossary that might be useful when using the fieldmap correction tools.

EPI-based fieldmap: measurement of the phase with EPI-sequence (results in distorted phase image)

fieldmap (FPM): calculated map of field inhomogeneity from the phase maps

Hertz (Hz): number of cycles per second (see chapter 12 of [29] on the Fast Fourier Transform)

receiver bandwidth (BW): $1/\delta t$

bandwidth (Hz) : Read-out bandwidth (BW_{RO}) is usually much higher than the effective bandwidth along the phase-encoded direction (BW_{PE}). For example, for a 0.5 ms echo spacing, the effective phase-encoding bandwidth is $\pm 1/(2 \times 0.5 \text{ ms}) = \pm 1 \text{ kHz}$, whereas the readout bandwidth is typically $\pm 100 \text{ kHz}$ or more [4, p.376].

dwelt time: The time between two successive samples (x-axis of k-space); determines highest frequency sampled accurately [30]. Dwell time = $1/\text{bandwidth}$. The resulting sampling time per complex point Δt (also known as the dwell time) is the inverse of the full readout bandwidth [4, p.367].

echo spacing The time between centers of two successive k-space lines.

asymtime: time difference of second pulse of symmetric and asymmetric spin-echo (SE), see figure D.1.

dwell-to-asymtime-ratio: dwelltime/asymtime, (usually between 0.2 and 0.3)(FSL).

Jacobian modulation: correction of intensity for expansion or compression of pixel (SPM).

polarity of phase encode blips or PE direction: phase encoding (PE) direction, usually the y-direction (x will be read-out (RO)) from posterior to anterior ($P \rightarrow A$). If the polarity is the reverse ($A \rightarrow P$), the polarity is negative.

magnitude image: this is the amplitude (complex modulus) of the signal (FSL: 'Abs' instead of 'Magn' (SPM)).

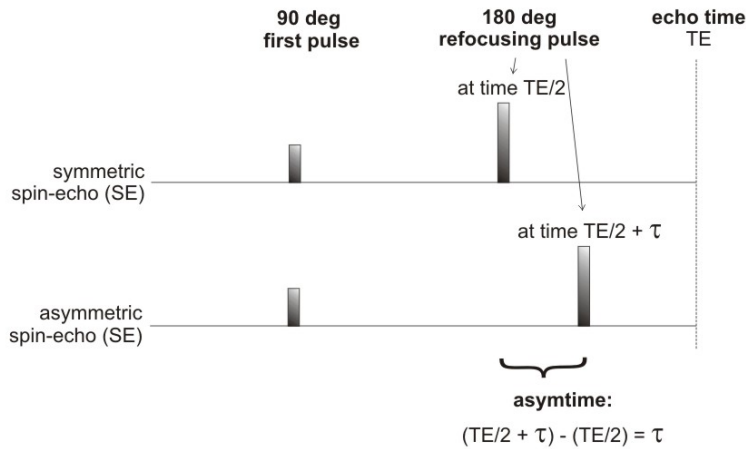


Figure D.1: asymtime: time difference of second pulse of symmetric and asymmetric spin-echo

phase image: phase part of complex signal, reflecting rotation angle; the other part is the magnitude. This is the polar representation of the real and imaginary values of a complex image.

total EPI readout time: number of echoes * echo spacing (SPM)

warped: geometrically distorted image

wrapped: concerns the imaginary part of complex data, representing rotation angles (phase). When there are phase jumps, i.e. when the phase is not gradually increasing but discontinuous, and when the phase is varying between $-\pi$ and π it is called *wrapped*. *Unwrapping* involves removing the phase jumps and adding multiples of π , so that the phases are not overlapping (multi-valued) but unique (single-valued).

Appendix E

Phase wraps and unwrapping

This section contains information from Ghiglia & Pritt (1998, [13]) and is just added for the interested reader and is not needed for use of the plugin.

Phase unwrapping in two dimensions essentially consists of detecting the pixel locations of the phase discontinuities, finding an ordering among the pixel locations for unwrapping the phase, and adding offsets of multiples of 2π .

According to Ghiglia & Pritt (1998, [13]), the two main approaches are *path following algorithms* and *minimum norm methods*. An overview of phase unwrapping methods is shown in figure E.1.

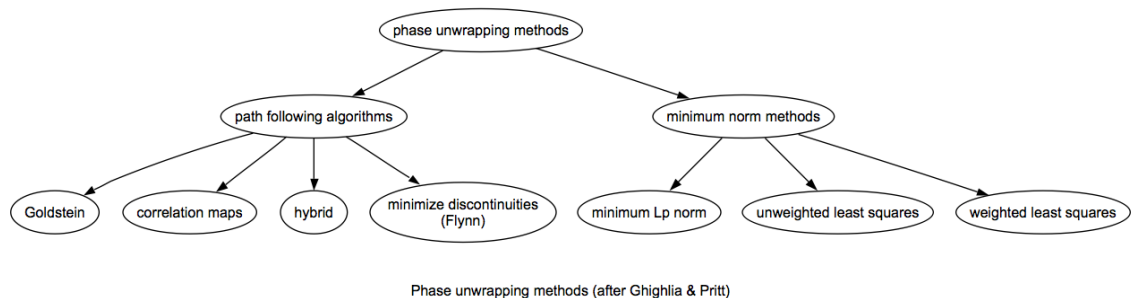


Figure E.1: Phase unwrapping methods classified by Ghiglia and Pritt (1998)

Path following algorithms

The path following algorithms find the residues and usually involve branch cuts to cope with the residues. A branch cut is a way to make a multi-valued complex function single-valued by imposing constraints on the possible paths a function can follow. In this way, the function can become single-valued which means that analytic methods can be used. The *residue* of a function at a singularity is the value of a function in a specific case [31, Ch.20]:

In case (i), $f(z)$ is of the form (20.67) and is described as having a pole of order p at $z = z_0$; the value of a_{-1} (not a_{-p}) is called the residue of $f(z)$ at the pole $z = z_0$ [...]. Finding the residue of a function at a singularity is of crucial importance in the evaluation of complex integrals.

Among the path following algorithms are *Goldstein's algorithm*, the use of *correlation maps*, *hybrid algorithms* and the *minimization of discontinuities* by Flynn (see left side of figure E.1). A branch cut approach for phase unwrapping of MRI images has been implemented by Cusack & Papadakis [9].

Minimum norm methods

The minimum norm methods that are used for phase unwrapping are the *minimum L_p norm*, *unweighted least squares* and *weighted least squares*.

The difference between the path following algorithms and the minimum norm methods is that [13, p.279]:

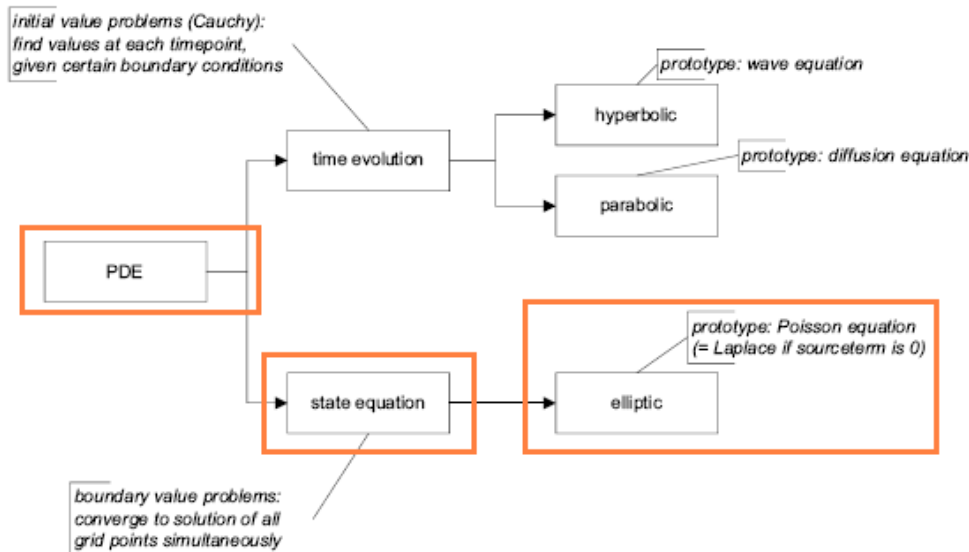
the path-following algorithms use localized operations that, in some sense, follow paths through the wrapped phase, while the minimum-norm algorithms take a more global approach that seeks to minimize some measure of the difference between the gradients of the wrapped phase and those of the solution.

There are different links between these very different approaches, of which one is a theorem that states that the solutions produced by the least squares algorithms are in some sense the averages of certain path-following solutions.

Minimum norm method: weighted 3D full multigrid (WFMG)

The goal is solving a discretised partial differential equation (PDE, see figure E; or elliptic equation) via the 3-dimensional multigrid method. This is a boundary value problem. This means that the boundary conditions have to be known in order to solve the equation by finding the values of the interior points (simultaneously).

PARTIAL DIFFERENTIAL EQUATION (PDE) TYPES



The weighted full multigrid (WFMG) method, which is used here for unwrapping, is a minimum norm method. A solution is generated, then the differences

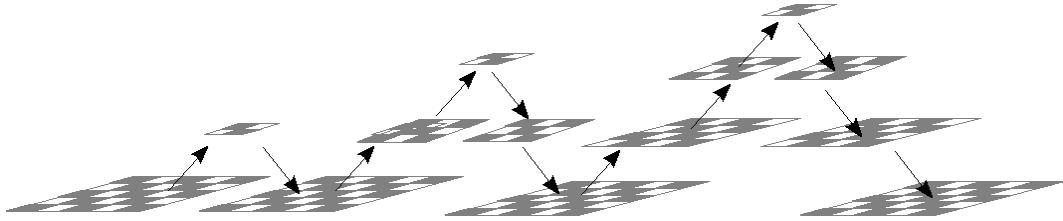


Figure E.2: Full multigrid (FMG): use an increasing number of grids to find a solution

between wrapped phase and the solution surface is minimized using least squares errors. This is performed by trying to find a solution on a coarse approximation of the data (see figure E.3). Because we use a quality map to indicate which data points are reliable, this is a *weighted* method. The effect of alternating between coarse and fine grid is a smooth solution, which makes additional noise removal in the fieldmap unnecessary.

Our method [6] is based on Press et al [29, Ch.19] and Gighlia & Pritt [13]. The difference with the first is that our method uses different boundary conditions and that the algorithm has been adapted for phase data. The difference with the latter is that our method is extended to 3D and uses different boundary conditions.

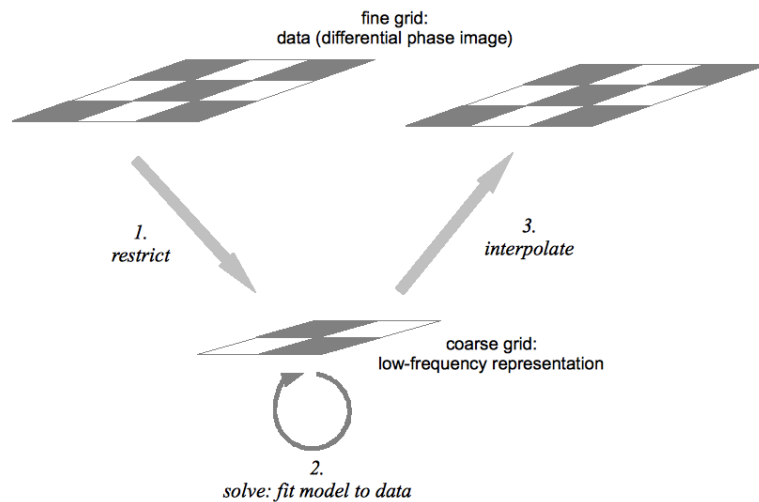


Figure E.3: V-cycle in multigrid method: from the fine grid, go to a coarse grid using a restriction operator (1), on the coarse grid, find a solution by minimizing the least square errors (2) and go back to the fine grid via interpolation (3)

For elaborate information about phase unwrapping, see Ghiglia & Pritt [13].

Bibliography

- [1] J.L.R. Andersson, S. Skare, and J. Ashburner. How to correct susceptibility distortions in spin-echo echo-planar images: application to diffusion tensor imaging. *NeuroImage*, 20:870–888, 2003.
- [2] P.B. Barker, K. Szopinski, and A. Horska. Metabolic heterogeneity at the level of the anterior and posterior commissures. *Magnetic Resonance in Medicine*, 43:348–354, 2000.
- [3] P.S.F. Bellgowan, P.A. Bandettini, P. van Gelderen, A. Martin, and J. Bodurka. Improved bold detection in the medial temporal region using parallel imaging and voxel volume reduction. *NeuroImage*, 29:1244–1251, 2006.
- [4] M.A. Bernstein, K.F. King, and X.J. Zhou. *Handbook of MRI Pulse Sequences*. Academic Press, 2004.
- [5] H. Breman, S. Frost, S. Okamoto-Barth, J. Peters, J. Zimmermann, C. Hutton, J. Ashburner, N. Weiskopf, and R. Goebel. Quantifying the effect of the susceptibility artifact on volume and surface. In *Presented at the OHBM meeting in Barcelona, Spain.*, 2010.
- [6] H. Breman, J. Peters, J. Ashburner, N. Weiskopf, and R. Goebel. Fast fieldmap-based epi distortion correction with anatabacus: a plugin for brainvoyager. *NeuroImage*, 47(Supplement 1):S81, July 2009.
- [7] N.K. Chen, C.C. Dickey, S.S. Yoo, C.R.G. Guttmann, and L.P. Panych. Selection of voxel size and slice orientation for fmri in the presence of susceptibility field gradients: application to imaging of the amygdala. *NeuroImage*, 19:817–825, 2003.
- [8] R. Cusack, M. Brett, and K. Osswald. An evaluation of the use of magnetic field maps to undistort echo-planar images. *NeuroImage*, 18(1):127–142, 2003.
- [9] R. Cusack and N. Papadakis. New robust 3-d phase unwrapping algorithms: Application to magnetic field mapping and undistorting echo-planar images. *NeuroImage*, 16:754–764, 2002.
- [10] R. Cusack, B. Russell, S.M.L. Cox, C. De Panfilis, C. Schwarzbauer, and R. Ansonge. An evaluation of the use of passive shimming to improve frontal sensitivity in fmri. *NeuroImage*, 24:82–91, 2005.
- [11] J.T. Devlin, R.P. Russell, M.H. Davis, C.J. Price, J. Wilson, H.E. Moss, P.M. Matthews, and L.K. Tyler. Susceptibility-induced loss of signal: Comparing pet and fmri on a semantic task. *NeuroImage*, 11:589–600, 2000.
- [12] J.C. Dreher, P. Kohn, and K.F. Berman. Neural coding of distinct statistical properties of reward information in humans. *Cerebral Cortex*, 16:561–573, 2006.

- [13] D.C. Ghiglia and M.D. Pritt. *Two-Dimensional Phase Unwrapping. Theory, Algorithms and Software*. New York: John Wiley and Sons, Inc, 1998.
- [14] G.H. Glover and C.S. Law. Spiral-in/out bold fmri for increased snr and reduced susceptibility artifacts. *Magnetic Resonance in Medicine*, 46:515–522, 2001.
- [15] R. Goebel, F. Esposito, and E. Formisano. Analysis of fiac data with brainvoyager qx: From single-subject to cortically aligned group glm analysis and self-organizing group ica. *Human Brain Mapping*, 27(5):392–401, 2006.
- [16] M.L. Gorno-Tempini, C. Hutton, O. Josephs, R. Deichmann, C. Price, and R. Turner. Echo time dependence of bold contrast and susceptibility artifacts. *NeuroImage*, 15, 2002.
- [17] K.A. Heberlein and X. Hu. Improved shim by changing head position. In *Proceedings of the 9th Annual Meetings ISMRM, Glasgow UK*, pages 1157–1157, 2001.
- [18] C. Hutton, A. Bork, O. Josephs, R. Deichmann, J. Ashburner, and R. Turner. Image distortion correction in fmri: A quantitative evaluation. *NeuroImage*, 16(1):217–240, 2001.
- [19] C. Hutton, R. Deichmann, R. Turner, and J.L.R. Andersson. Combined correction for geometric distortion and its interaction with head motion in fmri. In *Proceedings of ISMRM 12, Kyoto, Japan*, 2004.
- [20] C. Hutton, M.L. Gorno-Tempini, O. Josephs, R. Deichmann, C. Price, and R. Turner. Echo time dependence of bold contrast and susceptibility artifacts. *NeuroImage*, 13(6):S19–S19, 2001.
- [21] M. Jenkinson. Coordinate transformation conventions for spatial registration. Origin and date of document unknown.
- [22] P. Jezzard and B.S. Balaban. Correction for geometric distortion in echo planar images from b0 field variations. *MRM*, 34(1):65–73, 1995.
- [23] P.H.H. Leijendeckers, J.B. Fortuin, F. van Herwijnen, and G.A. Schwippert, editors. *Poly-Technisch Zakboek*. Doetinchem: Reed Business Information bv, 50e druk edition, 2003.
- [24] T.Q. Li, A. Takahashi, Y. Wang, V. Mathews, and G.H. Glover. Dual-echo spiral in/in acquisition method for reducing magnetic susceptibility artifacts in blood-oxygen-level-dependent functional magnetic resonance imaging. *Magnetic Resonance in Medicine*, 55:325–334, 2006.
- [25] K.D. Merboldt, P. Fransson, H. Bruhn, and J. Frahm. Functional mri of the human amygdala? *NeuroImage*, 14:253–257, 2001.
- [26] B. Nijdam and H. van Buuren. *Statistiek voor de sociale wetenschappen*, volume Deel I en II. Alphen aan den Rijn/Zaventem: Samsom Bedrijfsinformatie, 1994.
- [27] R.A. Oesterbauer, J.L. Wilson, G.A. Calvert, and P. Jezzard. Physical and physiological consequences of passive intra-oral shimming. *NeuroImage*, 29:245–253, 2006.
- [28] W.G. Ojemann, E. Akbudak, A.Z. Snijder, R.C. McKinstry, M.E. Raichle, and T.E. Conturo. Anatomic localization and quantitative analysis of gradient refocused echo-planar fmri susceptibility artifacts. *NeuroImage*, 6:156–167, 1997.

- [29] W.A. Press, S.A. Teukolsky, W.T. Vetterling, and B.P. Flannery. *Numerical Recipes in C; The Art of Scientific Computing*. Cambridge: Cambridge University Press, 2002.
- [30] S.S. Rajan. *MRI; a conceptual overview*. New York: Springer-Verlag, 1997.
- [31] K.F. Riley, M.P. Hobson, and S.J. Bence. *Mathematical Methods for Physics and Engineering*. Cambridge, UK: Cambridge University Press, 1998.
- [32] S.W. Smith. *The Scientist and Engineer's Guide to Digital Signal Processing*. California Technical Publishing, 1997. See <http://www.dspguide.com/>.
- [33] T. Stoecker, T. Kellermann, F. Schneider, U. Habel, K. Amunts, P. Pieperhoff, K. Zilles, and N.J. Shah. Dependence of amygdala activation on echo time: Results from olfactory fmri experiments. *NeuroImage*, 30:151–159, 2006.
- [34] B.P. Sutton, D.C. Noll, and J.A. Fessler. Dynamic field map estimation using a spiral-in/spiral-out acquisition. *Magnetic Resonance in Medicine*, 51(6):1194–1204, 2004.
- [35] P. Thevenaz, T. Blu, and M. Unser. Interpolation revisited. *IEEE Transactions on Medical Imaging*, 19(7):739–758, 2000.
- [36] N. Weiskopf, C. Hutton, O. Josephs, and R. Deichmann. Optimal epi parameters for reduction of susceptibility-induced bold sensitivity losses: A whole-brain analysis at 3 t and 1.5 t. *NeuroImage*, 33(2):493–504, 2006.
- [37] J.L. Wilson, M. Jenkinson, and P. Jezzard. Optimization of static field homogeneity in human brain using diamagnetic passive shims. *Magnetic Resonance in Medicine*, 48:906–914, 2002.